The LINNEAN SOCIETY of London ZOOLOGICAL Journal of the Linnean Society

Zoological Journal of the Linnean Society, 2015, **173**, 190–216. With 11 figures

Taxonomic status and phylogenetic relationships of *Marmosa agilis peruana* Tate, 1931 (Didelphimorphia: Didelphidae), with comments on the morphological variation of *Gracilinanus* from central–western Brazil

THIAGO BORGES FERNANDES SEMEDO[1]*, MARCUS VINICIUS BRANDÃO[2], ANA PAULA CARMIGNOTTO[2], MARIO DA SILVA NUNES[3], IZENI PIRES FARIAS[3], MARIA NAZARETH FERREIRA DA SILVA[4] and ROGÉRIO VIEIRA ROSSI[1]

[1]*Universidade Federal de Mato Grosso, Instituto de Biociências, Cuiabá, Mato Grosso, Brazil*
[2]*Universidade Federal de São Carlos, Campus Sorocaba, Departamento de Biologia, Laboratório de Diversidade Animal, Sorocaba, São Paulo, Brazil*
[3]*Universidade Federal do Amazonas, Departamento de Biologia, Laboratório de Evolução e Genética Animal (LEGAL), Manaus, Amazonas, Brazil*
[4]*Instituto Nacional de Pesquisas da Amazônia, Coleção de Mamíferos, Manaus, Amazonas, Brazil*

Received 19 March 2014; revised 17 July 2014; accepted for publication 21 August 2014

The marsupials of the family Didelphidae went through profound taxonomic rearrangements in recent decades, mainly related to an increase in the number of specimens deposited in scientific collections and the inclusion of molecular data in systematic analyses, resulting in better resolved phylogenies and taxa delimitation. Analyses of a large series of the gracile mouse opossum *Gracilinanus agilis*, including types and complementary material, recovered specimens assignable to *Marmosa agilis* peruana Tate, 1931 as a monophyletic group that is diagnosable by unique morphological, morphometric and molecular datasets, meriting its recognition as a full species. Here we provide an emended diagnosis, description and comparisons with congeners for *G. peruanus*. The former species differs from the latter by the dull reddish dorsal pelage, smaller general size, position of the maxillary fenestrae, presence of accessory cusps in upper canines, and morphology of the alisphenoid tympanic process. It ranges from central Peru to central Bolivia and western Brazil in the states of Rondônia and northwestern Mato Grosso, where it occurs in sympatry with *G. agilis*. Many collecting localities lie in areas with high diversity of non-volant small mammals and accelerated deforestation processes, highlighting its importance in terms of biogeographic studies and conservation policies.

doi: 10.1111/zoj.12203

ADDITIONAL KEYWORDS: Cyt*b* – gracile mouse opossum – marsupial – mtDNA – phylogeny – South America – systematics – taxonomy.

INTRODUCTION

For the superficially similar small-bodied didelphid marsupials with dark masks surrounding the eyes and long prehensile tails, generally recognized as mouse opossums, Gardner & Creighton (1989) have elected five genera to encompass distinctive groups that were once gathered under the genus *Marmosa* (*sensu* Tate, 1933). Along with *Marmosa* Gray, 1821, *Marmosops* Matschie, 1916, *Micoureus* Lesson, 1842, and *Thylamys* Gray, 1843, *Gracilinanus* was proposed as a new genus by the aforementioned authors to account for Tate's (1933) *microtarsus* species group. Since then, the contents of

*Corresponding author. E-mail: thiagosemedo@gmail.com

Gracilinanus Gardner & Creighton, 1989 have changed drastically. Hershkovitz (1992) provided the only revision of the genus, reporting nine valid species; however, in the first decade of the 21st century, several nominal taxa were recovered from the synonymies proposed by Hershkovitz (1992) and most of them were assigned to new genera, such as *formosa* Shamel, 1930, assigned to *Chacodelphys* by Voss, Tarifa & Yensen (2004); and *agricolai* Moojen, 1943, *chacoensis* Tate, 1931, *guahybae* Tate, 1931, *ignitus* Diaz, Flores & Barquez, 2002, and *unduaviensis* Tate, 1931, all assigned to *Cryptonanus* by Voss, Lunde & Jansa (2005). In addition, *kalinowskii* Hershkovitz, 1992 was assigned to *Hyladelphys* by Voss, Lunde & Simmons (2001). Therefore, as currently defined, the genus *Gracilinanus* is composed of six valid species: *Gracilinanus aceramarcae* (Tate, 1931); *Gracilinanus agilis* (Burmeister, 1854); *Gracilinanus dryas* (Thomas, 1898); *Gracilinanus emiliae* (Thomas, 1909); *Gracilinanus marica* (Thomas, 1898); and *Gracilinanus microtarsus* (Wagner, 1842) (Voss & Jansa, 2009).

Species of *Gracilinanus* are small, arboreal opossums restricted to tropical and subtropical forested habitats in South America, ranging from Colombia to south-eastern Brazil, northern Uruguay, and the Province of Misiones, Argentina (D'Elía & Martínez, 2006; Teta *et al*., 2007; Creighton & Gardner, 2008). The genus range also includes eastern Panama (Voss, Fleck & Jansa, 2009: table 4). Three species are known to occur in Brazil: *G. agilis*, from moist and dry forests of central Brazil; *G. emiliae*, from lowland rainforests and also along gallery forests within some savanna-dominated landscapes in central and northern South America; and *G. microtarsus*, from the Atlantic rainforest (Creighton & Gardner, 2008; Voss *et al*., 2009; Lóss, Costa & Leite, 2011).

Among the Brazilian species, *G. emiliae* is the most distinctive of the genus, being easily distinguished from its counterparts by diagnostic morphological traits such as warm reddish brown dorsal pelage, completely self-white underparts, and a distinctively longer tail (Voss *et al*., 2009). Regarding cranial morphology, this species exhibits a beaded interorbital region, has small or absent maxillary fenestrae, and consistently presents posterior accessory cusps in the upper canines (Voss *et al*., 2009).

The other two species in Brazil, which are morphologically similar and occur in sympatry in a few localities within their geographic distribution, only recently had their taxonomic status clarified by Costa, Leite & Patton (2003). It had been suggested that *G. agilis* could be a conspecific or even a subspecies of *G. microtarsus* (see Hershkovitz, 1992; Gardner, 1993); however, Costa *et al*. (2003) provided morphological and molecular evidence that these taxa should be treated as distinct species (14.9% of mean genetic distance based on mitochondrial cytochrome *b*, Cyt*b*, sequences). *Gracilinanus agilis* differs from *G. microtarsus* by a combination of external and craniodental traits. Externally, *G. agilis* exhibits greyish brown dorsal pelage, whereas *G. microtarsus* is chestnut brown; ventrally, *G. agilis* and *G. microtarsus* are quite similar, with grey-based hairs and buff underparts, only differing by the extension of the grey-based hairs, which cover the ventral surface from the throat to the anus in *G. microtarsus*, but extend from the lower chest to the anus in *G. agilis*. *Gracilinanus microtarsus* also exhibits a marked colour change between the muzzle and dorsum, and a wide, blackish circumocular mask, versus a gradual colour change and narrow mask in *G. agilis* (Costa *et al*., 2003).

The craniodental characters in *G. agilis* and *G. microtarsus* are very similar, but they can be distinguished by the posterolateral palatal foramina being larger than the palatine fenestra in *G. agilis* versus smaller in *G. microtarsus*, and by subequal upper premolars (P2 and P3) in *G. agilis* versus P2 being distinctly taller than P3 in *G. microtarsus* (Costa *et al*., 2003). In addition, *G. microtarsus* has longer tooth rows, broader and shorter pterygoids, proportionally greater breadth across the pars petrosa, longer skulls, wider braincase, wider zygomatic arch, and a broader interorbital region (Costa *et al*., 2003).

Regarding genetic diversity, Costa *et al*. (2003) reported high levels of genetic divergence within *G. microtarsus* (9.6% in Cyt*b* sequences) suggesting a species complex; however, this was not confirmed by subsequent morphological analysis (Lóss *et al*., 2011). By contrast, these authors found low genetic divergence (3.9% for Cyt*b*) between clades of *G. agilis* from central, north-eastern, and eastern Brazil, not supporting more than one taxon in the species. Similar results were recently found by Faria *et al*. (2013) based on two molecular markers (Cyt*b* and exon 28 of the nuclear von Willebrand Factor, vWF) and a larger number of specimens, but representing the same geographical range as described in the previous studies.

The samples studied by Faria *et al*. (2013) encompass localities of several nominal taxa currently considered as junior synonyms of *G. agilis*, such as *Marmosa beatrix* Thomas, 1910 and *Marmosa blaseri* Miranda-Ribeiro, 1936, but not others, such as *Marmosa agilis buenavistae* Tate, 1931, *Marmosa agilis peruana* Tate, 1931, and *Thylamys rondoni* Miranda-Ribeiro, 1936 (Creighton & Gardner, 2008; Voss & Jansa 2009). Indeed, the latter nominal taxa were described based on specimens from central–western Brazil, an area that represents a significant portion of the geographic distribution of *G. agilis* and from where no samples had been included in previous genetic studies. In this sense, the question of whether *G. agilis* represents a single taxonomic unit or a species complex remains

unresolved until representative samples from the entire geographic range of this taxon are included. Creighton & Gardner (2008) have previously stressed this point when observing the variation in pelage coloration within *G. agilis*, which ranges from dusky grey to dull reddish brown, stating that this group urgently needs a revision.

In this paper, we describe the morphological and genetic variation in specimens of *Gracilinanus* from central–western Brazil, and propose that *Marmosa agilis peruana* Tate, 1931, currently regarded as a junior synonym of *G. agilis*, be elevated to the full species category.

MATERIAL AND METHODS

Molecular analyses

Samples

Partial sequences of the mitochondrial Cyt*b* gene (801 bp) were obtained for 20 specimens identified by the authors as *G. agilis* from western Mato Grosso state, Brazil (Fig. 1). In addition, we downloaded available sequences from GenBank (http://www.ncbi.nlm.nih.gov/GenBank/) representing the other valid species of *Gracilinanus*, such as *G. aceramarcae*, *G. emiliae*, and *G. microtarsus* (Fig. 1). We also obtained sequences from GenBank of *Cryptonanus unduaviensis*, *Marmosops impavidus* (Tschudi, 1845), and *Marmosa murina* (Linnaeus, 1758) for use as out-groups, and to root the trees in our phylogenetic analyses (Table 1). Out-group taxa were chosen based on the phylogenetic results of Voss & Jansa (2009). The sequences obtained in this study are deposited in GenBank under the following accession numbers: KM066014–KM066033.

Laboratory procedures

DNA was extracted from ethanol-preserved tissues using phenol-chloroform and proteinase K RNase methods (Sambrook, Ritsch & Aniatis, 1989). The sequences were amplified by polymerase chain reaction (PCR) using primers: GluMarsF1 (5′-AACCATAACCTATGGCATGAA-3′) and CytbMarsR2 (5′-GTGGAAKGCRAARAATCGDGT-3′). The PCR analysis was performed with a final volume of 13 μL, comprising the following: 5.2 μL of H_2O; 1.5 μL of $MgCl_2$ (2.5 mM); 1.25 μL of dNTP (2.5 mM); 1.25 μL of 10× buffer (100 mM Tris-HCl, 500 mM KCl); 1 μL of forward primer (0.2 μM); 1 μL of reverse primer (0.2 μM); 0.8 μL of Taq DNA polymerase (1 U μL^{-1}); and 1 μL of genomic DNA. PCR conditions used a pre-heating step of 94 °C for 1 min, followed by 35 cycles of 94 °C for 1 min, 55 °C for 1.30 min, 1 minute at 72 °C, and a final extension at 72 °C for 10 min. PCR products were cleaned using Exonuclease I and Shrimp Alkaline Phosphatase (Fermentas), and sequenced using automatic sequencer ABI 3130xl Genetic Analyzer (Life Technologies).

Sequence alignments and phylogenetic analyses

The partial Cyt*b* sequences, which did not show any insertions or deletions (indels), were manually edited with BioEdit 7.1 (Hall, 1999) and confirmed by translating the DNA data into putative amino acid sequences. Diagnostic sites for each taxon were identified in the R package SPIDER (Brown *et al*., 2012). We used jModelTest (Posada, 2009) to determine the best model of sequence evolution that fits the evolutionary parameter values for the data. We determined the transitional model with the γ parameter (TIM+G; Posada, 2006) to be the most likely model of sequence evolution, selected via the Akaike information criterion (AIC). Maximum-likelihood (ML) phylogenetic analysis was performed using the program Treefinder (Jobb, von Haeseler & Strimmer, 2004), and Bayesian inference (BI) phylogenetic analysis was performed using the program MrBayes 3.2 (Ronquist *et al*., 2012) under the TIM+G model of molecular evolution. We also conducted maximum parsimony analysis (MP) in PAUP* 4.0b10 (Swofford, 2002) using a heuristic search and the tree bisection and reconnection (TBR) branch-swapping algorithm. Nonparametric bootstrapping based on 1000 replicates was performed for both analyses. Mean Kimura 2-parameter (K2P; Kimura, 1980) distances within and between groups were calculated in MEGA 5.0 (Tamura *et al*., 2011). The K2P model was chosen to allow comparison with divergence estimates reported in previously published studies involving *Gracilinanus* species (Lóss *et al*., 2011; Faria *et al*., 2013).

Morphological and morphometric analyses

Samples

We examined a total of 194 specimens (Appendix), including holotypes, paralectotypes, topotypes, and important complementary material in the genus *Gracilinanus* (Fig. 1). The examined material comprised either skin and skull, fluid preserved and skull, or only fluid-preserved specimens, deposited in the following collections (listed with their standard institutional abbreviations): American Museum of Natural History, New York, USA (AMNH); Natural History Museum, London, UK (BMNH); Coleção de Mamíferos da Universidade Estadual de Mato Grosso, Campus de Nova Xavantina, Nova Xavantina, Brazil (CM); Instituto Nacional de Pesquisa da Amazônia, Manaus, Brazil (INPA); Museu Nacional, Universidade Federal do Rio de Janeiro, Rio de Janeiro, Brazil (MN); Museo Noel Kempff Mercado, Santa Cruz, Bolivia (MNK); Museu Paraense Emílio Goeldi, Belém, Brazil (MPEG); Museu de Zoologia da Universidade de São Paulo, São Paulo, Brazil (MZUSP); Coleção Zoológica da Universidade Federal de Mato Grosso, Cuiabá, Brazil (UFMT), and Universidade Federal da Paraíba, João

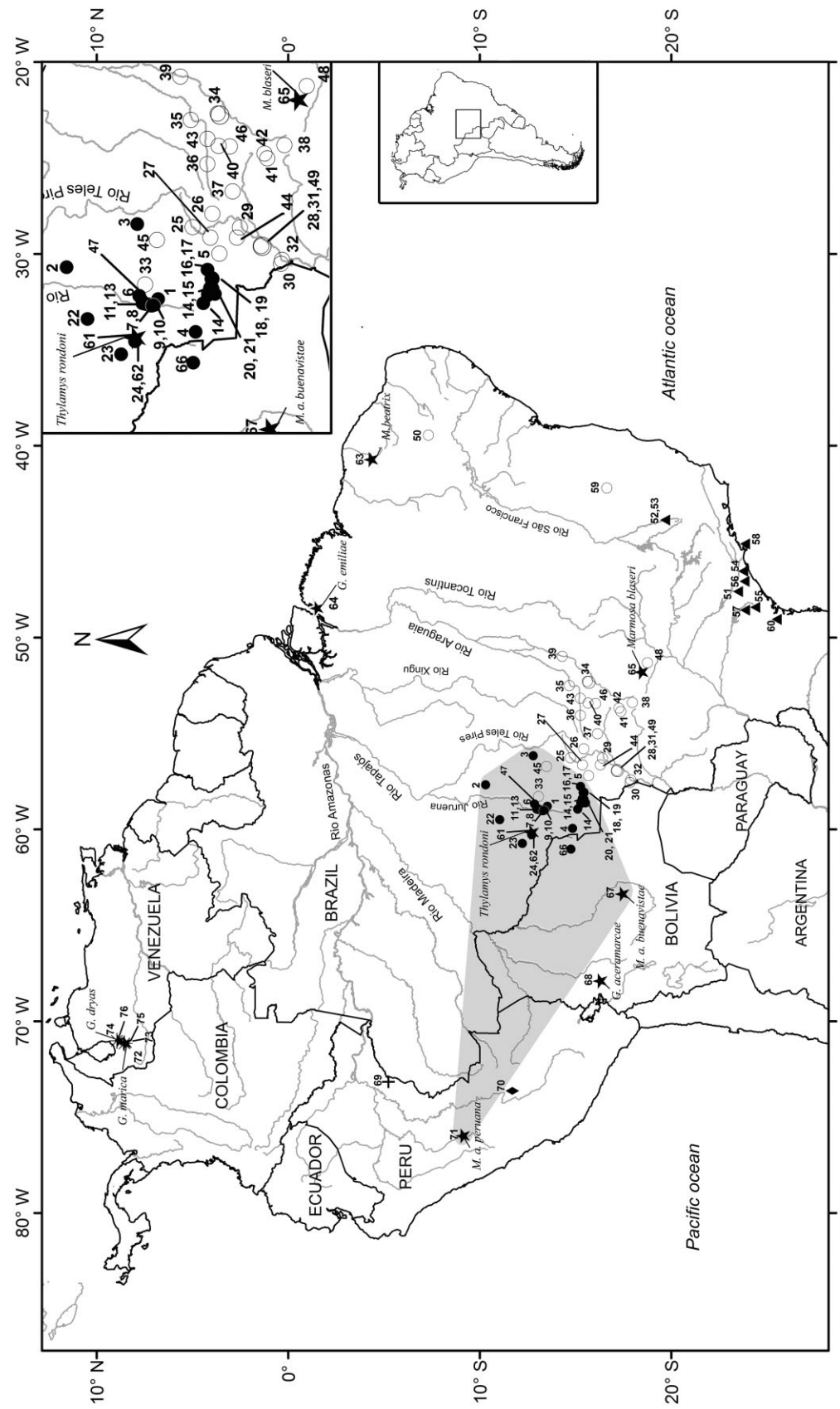

Figure 1. Map of the distribution localities of *Gracilinanus* specimens included in phylogenetic and/or morphological analyses in the present study. Numbers correspond to the localities listed in the Appendix; •, *Gracilinanus peruanus*; ○, *Gracilinanus agilis*; ★, type material associated with *Gracilinanus*. Records based on sequenced specimens taken from GenBank used in the phylogenetic analyses are as follows: ▲, *Gracilinanus microtarsus*; +, *Gracilinanus emiliae*; ◆, *Gracilinanus aceramarcae*; *, *Gracilinanus dryas* (see Table 1 and Appendix). The shaded area corresponds to the *G. peruanus* distribution based on this study.

Table 1. List of sequenced specimens included in the molecular analyses of cytochrome *b*

Species	Voucher number	GenBank accession number	Locality (numbers)	Reference
Gracilinanus aceramarcae	MUSM 13002	HQ622162	Peru: Junín, Cordillera de Vilcabamba (68)	Lóss *et al*. (2011)
Gracilinanus agilis	MZUSP 35186	KM066018	BR: MT, Parna Pantanal (32)	This study
Gracilinanus agilis	MZUSP 35187	KM066017	BR: MT, Parna Pantanal (32)	This study
Gracilinanus agilis	MZUSP 35188	KM066022	BR: MT, Parna Pantanal (32)	This study
Gracilinanus agilis	MZUSP 35190	KM066021	BR: MT, Parna Pantanal (32)	This study
Gracilinanus agilis	MZUSP 35191	KM066020	BR: MT, Parna Pantanal (32)	This study
Gracilinanus agilis	MZUSP 35192	KM066016	BR: MT, Parna Pantanal (32)	This study
Gracilinanus agilis	UFMT 2043	KM066019	BR: MT, Fazenda Eldorado (34)	This study
Gracilinanus agilis	UFMT 1039	KM066025	BR: MT, Margem esquerda do Rio Cumbuco (36)	This study
Gracilinanus agilis	UFMT 3818	KM066015	BR: MT, Jaciara/Jucumeira (37)	This study
Gracilinanus agilis	UFMT 3817	KM066014	BR: MT, Jaciara/Jucumeira (37)	This study
Gracilinanus agilis	CM 598	KM066024	BR: GO, Alta Cachoeira (48)	This study
Gracilinanus agilis	UFMT 3892*	KM066023	Mato Grosso, Brazil	This study
Gracilinanus agilis	UFMG 2497	HQ622159	BR: MT, Base de Pesquisas do Pantanal (49)	Lóss *et al*. (2011)
Gracilinanus agilis	UFMG 2504	HQ622149	BR: CE, Chapada do Araripe (50)	Lóss *et al*. (2011)
Gracilinanus agilis	UFMG 2495	HQ622155	BR: MG, Ponte do Colatino (59)	Lóss *et al*. (2011)
Gracilinanus emiliae	MUSM 15292	HM583367	Peru: Nuevo San Juan, Rio Galvez (69)	Giarla *et al*. (2010)
Gracilinanus microtarsus	UFMG 2537†	HQ622166	BR: SP, Floresta Nacional de Ipanema (51)	Lóss *et al*. (2011)
Gracilinanus microtarsus	MHNCI 2793	HQ622163	BR: PR, Piraquara (60)	Lóss *et al*. (2011)
Gracilinanus microtarsus	MN 31445	HQ622173	BR: MG, Lagoa Santa (52)	Lóss *et al*. (2011)
Gracilinanus peruanus	INPA 6741	KM066033	BR: MT, Fazenda Quatro Meninas (14)	This study
Gracilinanus peruanus	INPA 6740	KM066029	BR: MT, Fazenda Água Limpa (15)	This study
Gracilinanus peruanus	INPA 6739	KM066028	BR: MT, Fazenda Araputanga (16)	This study
Gracilinanus peruanus	INPA 6738	KM066030	BR: MT, Fazenda Araputanga (16)	This study
Gracilinanus peruanus	INPA 6737	KM066032	BR: MT, Fazenda Alto Jauru (18)	This study
Gracilinanus peruanus	INPA 6736	KM066031	BR: MT, Fazenda Alto Jauru (18)	This study
Gracilinanus peruanus	UFMT 1379	KM066027	BR: MT, Serra do Expedito (22)	This study
Gracilinanus peruanus	UFMT 3816	KM066026	BR: RO, Chupinguaia (23)	This study
Cryptonanus unduaviensis	AMNH 262401	HM583366	BO: Pando, Independencia‡	Giarla *et al*. (2010)
Marmosops impavidus	MSB 57002	HM583368	BO: Pando, Palmira‡	Giarla *et al*. (2010)
Marmosa murina	MVZ 197421	HM106391	BR: MT, Fazenda São Luís‡	Gutiérrez *et al*. (2010)

For each species, the voucher number, GenBank accession number, and locality is provided; Brazilian (BR) states are CE (Ceará), GO (Goiás), MG (Minas Gerais), MT (Mato Grosso), PR (Paraná), RO (Rondônia), SP (São Paulo), and BO for (Bolivia). The acronyms of the scientific institutions are as follows: MHNCI: Museu de História Natural Capão da Imbuia, Curitiba; MSB: Museum of Southwestern Biology, Albuquerque; MUSM: Museo de Historia Natural de la Universidad Nacional Mayor de San Marcos, Lima; MVZ: Museum of Vertebrate Zoology, Berkeley; UFMG: Universidade Federal de Minas Gerais, Belo Horizonte. See the Appendix for the locality names and locality numbers plotted on the map (Fig. 1).

*Specimen of *Gracilinanus agilis* from Mato Grosso state, Brazil, with no specific locality.

†Specimen from the type locality of *Gracilinanus microtarsus* (Lóss *et al*., 2011).

‡For locality, see Giarla *et al*. (2010) and Gutiérrez *et al*. (2010); these were not shown on the map of Figure 1.

Pessoa, Brazil (UFPB). We also analysed uncatalogued specimens collected by Manoel dos Santos Filho (field acronym MSF) that will be deposited in INPA and the Universidade Estadual de Mato Grosso, Campus de Cáceres, Cáceres, Brazil (UNEMAT).

The types of nominal taxa that were analysed under the *G. agilis* complex were *Marmosa beatrix* Thomas, 1910 (holotype BMNH 11.4.23.24, skin/skull), *Marmosa agilis buenavistae* Tate, 1931 (holotype BMNH 26.12.4.91, skin/skull), *Marmosa agilis peruana* Tate, 1931 (holotype BMNH 27.11.1.268, skin/skull, and topotype BMNH 27.11.1.269, skin/skull), *Marmosa blaseri* Miranda-Ribeiro, 1936 (holotype MN 1250, skin/skull), and *Thylamys rondoni* Miranda-Ribeiro, 1936 (paralectotype MN 1276, skin/skull). We also examined the types of four currently valid species: *Gracilinanus aceramarcae* (Tate, 1931) (AMNH 72568, skin/skull), *Gracilinanus dryas* (Thomas, 1898) (BMNH 98.5.15.2, skin/skull), *Gracilinanus emiliae* (Thomas, 1909) (BMNH 9.3.9.10, skin/skull), and *Gracilinanus marica* (Thomas, 1898) (BMNH 98.5.15.1, skin/skull). Although the holotype of *Gracilinanus agilis* (Burmeister, 1854), deposited at the Zoologisch Museum, Halle, Germany, was not examined, we used the original description (Burmeister, 1854) and the description of Tate (1933) for reference.

Comparative analyses of external and craniodental morphology were performed by examination of the

material to hand (skin/skull and fluid). We examined the following characters: dorsal and ventral pelage coloration; tail coloration; morphology of tail scales and hairs; extension of rostral bones; patterns of the supraorbital margins; patterns of palatal fenestrae; morphology of the bones and patterns of the secondary foramen ovale (represented by the anteromedial process of the alisphenoid tympanic wing) in the auditory region; and presence of accessory cusps on the upper canines. We gave priority to comparisons among specimens of the same sex and age classes in order to avoid characters associated with sexual and age variation. Nomenclature for the external and craniodental morphology followed Voss & Jansa (2003, 2009).

Age criteria

The specimens were grouped into different age classes based on patterns of tooth eruption and exposure, using the classification proposed by Rossi, Voss & Lunde (2010b). To minimize ontogenetic variation, we only used adults (age classes 6–9) in the statistical analyses.

Measurements

For the specimens assigned to the *G. agilis* complex, we transcribed external body measurements (in millimetres) and mass (in grams) from museum labels as follows: total length (TL); length of head and body (HBL); length of tail (LT); length of hind foot (HF); and length of ear (Ear). For these specimens, we also took 25 craniodental measurements using a digital caliper recorded to the nearest 0.01 mm, whereas skulls were viewed at low magnification under a stereomicroscope. The dimensions are illustrated and based on the work of Rossi *et al*. (2010b: fig. 5). The measurements were as follows: greatest length of skull (GLS, from the anteriormost point of the premaxillae to the posteriormost point of the braincase at the supraoccipital); condylobasal length (CBL, from the occipital condyles to the anteriormost point of the premaxillae); rostral length (RL, from the anteriormost point of the nasals to the ventralmost lacrimal foramen); nasal length (NL, the greatest length of either the right or left nasal bone, whichever was longest); palatal length (PL, from the anteriormost point of the premaxillae to the posterolateral corner of the postpalatine torus); length of maxillary tooth row (MTR, from the anterior margin of the upper canine to the posterior margin of M4); length of upper molar series (UMS, crown length of the upper molars, from the anterolabial margin of M1 to the posterior margin of M4); length of M4 (LM4, length of the anteroposterior or mesiodistal dimension of the fourth upper molar crown across the paracone and metacone); width of M2 (WM2, transverse dimension of the second upper molar, from the labial margin of the crown at or near the stylar-A position to the lingual apex of the protocone); height of upper canine (HC, vertical dimension of C1, from the exposed labial base to the tip of the tooth); palatal breadth (PB, across the labial margins of M4 crowns); breadth across tympanic bullae (BTB, the greatest distance across the lateral margins of the right and left alisphenoid tympanic processes); length of tympanic bullae (LTB, from the anterior curvature of the alisphenoid tympanic process to the posteriormost point of the petrosal pars cochlearis); width of ectotympanic (WET, greatest width of the ectotympanic); nasal breadth (NB, across the triple-point sutures of the nasal, frontal, and maxillary bones on each side); breadth of rostrum across canines (BRC, across the labial bases of the upper canines); breadth of rostrum between jugals (BRJ, across the triple-point sutures of the jugal, lacrimal, and maxillary bones on each side); least interorbital breadth (LIB, at the narrowest point across the frontals between the orbits, anterior to the postorbital processes, if present); postorbital constriction (POC, at the narrowest point across the frontals between the temporal fossae, posterior to the postorbital processes, if present); breadth of braincase (BBC, from immediately above the zygomatic process of the squamosal on each side); zygomatic breadth (ZB, greatest breadth across the zygomatic arches); length of mandible (LM, from the anteriormost point of the mandible medial to the alveolus of i1 to the posteriormost point of the angular process); length of lower molar series (LMS, crown length of the lower molars, from the anterolingual margin of m1 to the posterolingual margin of m4); length of m4 (Lm4, anteroposterior or mesiodistal dimension of m4, from the paraconid to the hypoconulid); width of m2 (Wm2, transverse dimension of m2, measured across the hypoconid and entoconid).

Statistical analysis

Descriptive statistics were provided for the five external and 25 craniodental measurements. Preliminary analyses were performed to evaluate the normality using a Kolmogorov–Smirnov test (Sokal & Rohlf, 1981). To evaluate the sexual dimorphism in *G. agilis* and *G. peruanus* (herein recognized as a valid species; see Results section), we performed Student's *t*-tests in the craniodental dimensions. We also applied this test to evaluate which dimensions are significantly different between both species, considering males and females separately.

Principal component analysis (PCA) and discriminant analysis (DA) were performed to verify whether morphometric data were congruent with molecular and morphological data sets. In this sense, the specimens were identified a priori as *G. agilis* or *G. peruanus*, based on the morphological diagnostic qualitative traits and also on the molecular data (see Results). For both multivariate analyses, the entire data matrix was

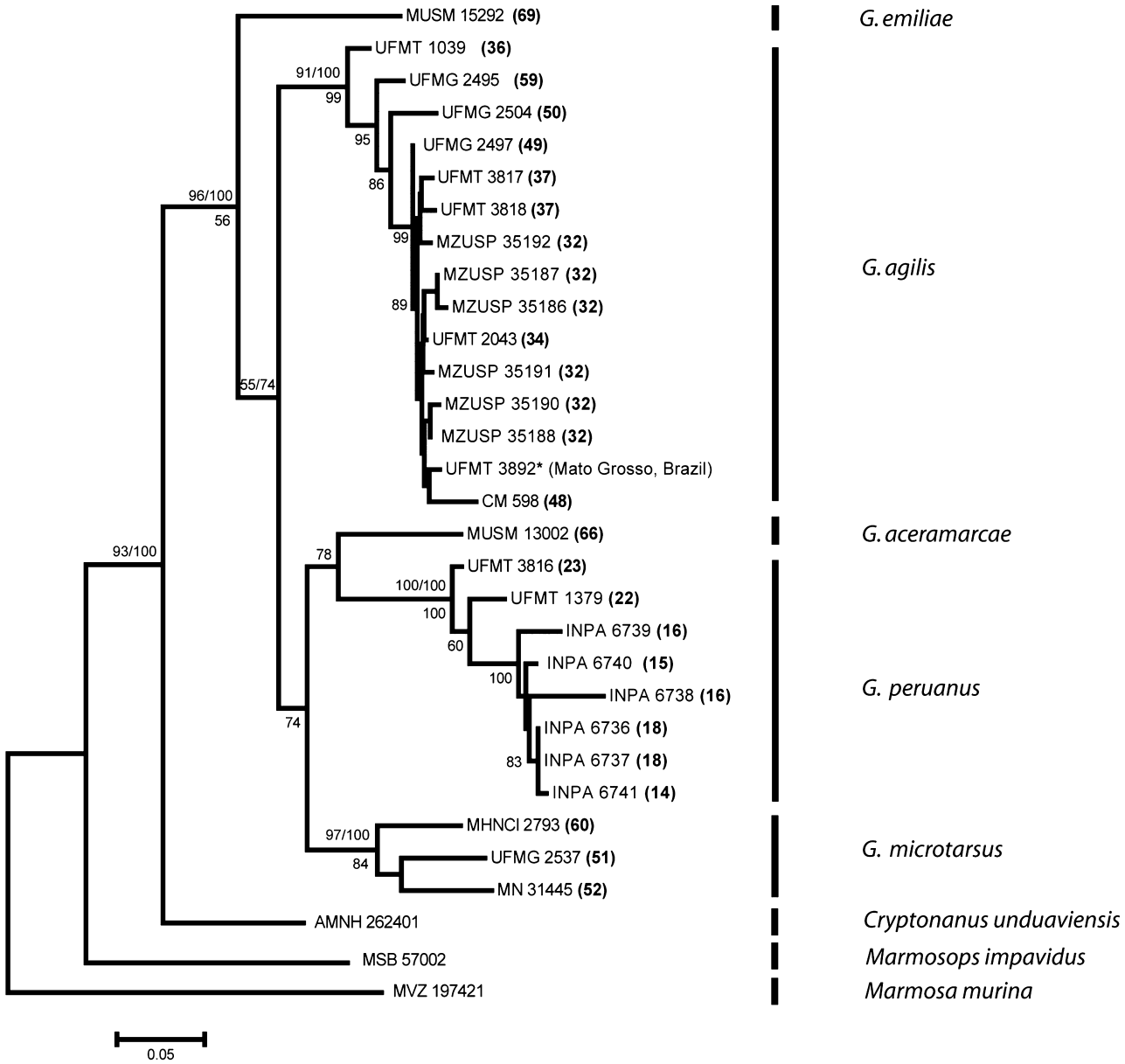

Figure 2. Maximum-likelihood phylogenetic hypothesis between specimens of *Gracilinanus* based on mtDNA cytochrome *b* data, obtained using the TIM+G model. The numbers to the left and right of the branches are posterior probability and bootstrap values for Bayesian inference (BI) and maximum-likelihood (ML) analyses, respectively. Bootstrap values for maximum-parsimony (MP) analysis are below the branches (only values > 50% are shown). Numbers refer to localities of specimens plotted in Figure 1 and listed in the Appendix. *Specimen of *Gracilinanus agilis* from Mato Grosso state, Brazil, with no specific locality.

normalized using log-transformations to reduce the effects of the magnitude of variables. For a closer comparison with holotypes, we did not include the cranial dimension ZB (see Measurements section) in PCA and DA, as some of the types had broken zygomatic arches. All statistical analyses considered a significance level at 5% and were performed using SPSS 13.0 for Windows.

RESULTS

MOLECULAR ANALYSIS

The alignment of the partial mitochondrial Cyt*b* gene (starting from the first base of the first codon position) resulted in 801 base pairs, of which 468 sites were conserved, 333 were variable, and 239 were parsimony informative. The topologies obtained for MP (not shown),

Table 2. Inter- and intraspecific mean pairwise genetic distances between species of *Gracilinanus* inferred using the Kimura two-parameter (K2P) evolutionary model

Taxon	Intergroup genetic distance					Intragroup genetic distance
	1	2	3	4	5	
1. *Gracilinanus emiliae*		0.022	0.020	0.023	0.020	
2. *Gracilinanus agilis*	0.168		0.019	0.020	0.018	0.023
3. *Gracilinanus aceramarcae*	0.143	0.136		0.019	0.017	
4. *Gracilinanus peruanus*	0.182	0.160	0.155		0.017	0.041
5. *Gracilinanus microtarsus*	0.159	0.142	0.129	0.153		0.090

Mean values are below the diagonal and standard deviations values are above the diagonal.

Table 3. Matrix of molecular synapomorphies of *Gracilinanus peruanus* in comparison with other analysed *Gracilinanus* species

Taxon	87	145	178	179	270	357	378	466	468	489
Gracilinanus aceramarcae	T	C	C	T	C	A	C	A	T	A
Gracilinanus agilis	T	C	C	T	C	A/T	C	A	C	A
Gracilinanus emiliae	T	C	C	T	C	A	C	A	T	A
Gracilinanus microtarsus	T	C	A/C	T	C	A	C	A	C/T	A
Gracilinanus peruanus	C	T	T	C	T	C	A/G	G	A	G

Column numbers indicate the position within the sequenced cytochrome *b* fragment obtained in the present study.

BI (not shown), and ML (Fig. 2) were similar in supporting the monophyly of the genus *Gracilinanus*, with support values of 56, 100, and 96%, respectively. *Gracilinanus emiliae* appears in all of the analyses as the sister taxon to all other species of *Gracilinanus*; however, Cyt*b* demonstrated limited resolution to recover the phylogenetic relationships between *Gracilinanus* species, particularly the relationships of *G. peruanus*, which exhibited conflicting results among the ML, MP (consensus of 11 most parsimonious trees, tree length = 534), and BI analyses. In the ML topology, *G. peruanus* appears as a sister taxon to *G. aceramarcae* (Fig. 2), and this clade in turn is related to *G. microtarsus*. In the MP consensus tree, there is a polytomy between all of the *Gracilinanus* species in which the phylogenetic relationships could not be fully resolved. In the BI phylogeny, *G. peruanus* appears as the sister species of the *G. aceramarcae* + *G. agilis* clade.

The mean genetic distance values between monophyletic groups that correspond to species ranged from 12.9% between *G. microtarsus* and *G. aceramarcae* to 18.2% between *G. peruanus* and *G. emiliae* (Table 2). The intraspecific mean genetic distance values ranged from 2.3% in *G. agilis* (15 specimens from ten distinct localities) to 9.0% in *G. microtarsus* (three specimens from three distinct localities). Comparisons involving genetic distances of *G. peruanus* ranged from 15.5% (with *G. aceramarcae*) to 18.2% (with *G. emiliae*). The molecular synapomorphies of *G. peruanus* compared with the other congeners are shown in Table 3. The analyses (MP, BI, and ML) recovered *G. peruanus* as a monophyletic group with a bootstrap value of 100% (Fig. 2).

Morphometric analyses

The descriptive statistics for adult specimens of *G. agilis* and *G. peruanus* herein examined are shown in Table 4. For comparisons, we also provide measurements of the following holotypes: *Marmosa agilis peruana* Tate, 1931, *M. a. buenavistae* Tate, 1931, and *M. beatrix* Thomas, 1910.

In general, males exhibited larger external and craniodental dimensions than females in both *G. agilis* and *G. peruanus* (Table 4). Among the craniodental dimensions, those related to the length of the skull (GLS, CBL, RL, NL, PL, and LM), the height of the canine (HC), the breadth of the rostrum across the jugals (BRJ), and the zygomatic breadth (ZB) were statistically different between males and females in both species. By contrast, the dimensions related to the upper and lower molars, the bullar region, and the pos-orbital constriction (POC) did not present sexual dimorphism. Twenty craniodental dimensions were significantly different between *G. agilis* and *G. peruanus* when considering males and females separately (Table 5).

Table 4. Descriptive statistics for external and craniodental dimensions (in millimetres) and mass (in grams) of adult specimens (age classes 6–9) of *Gracilinanus agilis*, *Gracilinanus peruanus*, and related holotypes

	Gracilinanus agilis		*Gracilinanus peruanus*				
					*M. a. peruana**	*M. beatrix*†	*M. a. buenavistae*‡
	Male	Female	Male	Female	Male	Female	Female
HBL	107.0 ± 18.2	97.3 ± 9.1	103.8 ± 8.4	95.6 ± 8.8	91.0	92.0	110.0
	85.0–120.0 (22)	80.0–112.0 (21)	92.0–121.0 (16)	85.0–115.0 (12)			
LT	139.7 ± 11.4	129.3 ± 13.2	145.1 ± 6.0	135.4 ± 4.5	136.0	125.0	140.0
	122.0–158.0 (28)	101.0–151.0 (21)	135.0–155.0 (16)	130.0–145.0 (12)			
HF	20.8 ± 1.8	20.6 ± 2.6	21.1 ± 1.7	20.2 ± 1.9	16.0	16.0	15.0
	17.5–23.7 (28)	14.9–25.0 (21)	17.0–24.0 (16)	17.0–24.0 (12)			
Ear	16.8 ± 2.9	15.8 ± 1.7	16.9 ± 1.0	16.1 ± 1.0	18.0	19.0	17.0
	11.0–25.5 (16)	13.8–21.0 (16)	15.0–19.0 (16)	14.0–17.0 (12)			
Mass	28.6 ± 4.7	22.8 ± 6.2	22.8 ± 7.4	19.3 ± 10.0	–	–	–
	20.0–34.0 (27)	12.0–41.0 (21)	12.0–39.0 (16)	10.0–49.0 (12)			
GLS	29.60 ± 1.00	28.3 ± 1.08	28.12 ± 0.94	26.66 ± 0.57	26.38	26.82	27.59
	27.88–32.00 (30)	26.32–30.45 (23)	26.35–29.48 (31)	25.05–27.76 (22)			
CBL	28.93 ± 1.15	27.35 ± 1.06	27.32 ± 1.02	25.78 ± 0.55	25.29	25.75	27.05
	27.06–31.56 (30)	25.47–29.52 (23)	25.37–28.91 (31)	24.50–26.85 (22)			
RL	10.90 ± 0.54	10.34 ± 0.63	10.16 ± 0.53	9.69 ± 0.41	9.24	9.16	10.17
	10.02–12.28 (30)	9.30–11.51 (23)	9.18–10.92 (26)	9.05–10.33 (20)			
NL	12.27 ± 0.65	11.70 ± 0.66	11.50 ± 0.5	10.84 ± 0.52	10.35	11.32	11.60
	10.65–13.70 (30)	10.76–13.48 (23)	10.57–12.25 (26)	9.30–11.73 (20)			
PL	15.51 ± 0.62	15.01 ± 0.58	15.05 ± 0.58	14.33 ± 0.39	13.74	14.22	15.11
	13.83–16.5 (31)	14.00–16.34 (23)	13.21–15.80 (31)	13.58–15.13 (22)			
MTR	10.77 ± 0.54	10.70 ± 0.32	10.42 ± 0.21	10.07 ± 0.18	9.89	9.95	10.37
	9.08–11.32 (30)	10.07–11.46 (23)	9.90–10.76 (31)	9.76–10.36 (22)			
UMS	5.62 ± 0.13	5.58 ± 0.14	5.28 ± 0.12	5.28 ± 0.10	5.18	5.20	5.22
	5.31–5.82 (32)	5.25–5.88 (23)	4.90–5.55 (31)	5.02–5.46 (22)			
LM4	0.84 ± 0.07	0.81 ± 0.07	0.72 ± 0.06	0.70 ± 0.05	0.67	0.84	0.83
	0.71–0.96 (29)	0.71–1.02 (23)	0.62–0.90 (31)	0.62–0.82 (20)			
WM2	1.64 ± 0.07	1.62 ± 0.11	1.53 ± 0.06	1.53 ± 0.07	1.61	1.55	1.55
	1.43–1.80 (32)	1.25–1.80 (23)	1.38–1.68 (31)	1.26–1.62 (22)			
HC	2.19 ± 0.24	1.96 ± 0.19	2.24 ± 0.26	1.95 ± 0.16	2.57	1.38	2.29
	1.70–3.08 (31)	1.61–2.37 (23)	1.82–2.98 (31)	1.61–2.51 (22)			
PB	9.06 ± 0.31	8.86 ± 0.35	8.25 ± 0.32	8.11 ± 0.23	7.92	8.17	8.36
	8.47–9.62 (30)	8.25–9.71 (23)	7.46–8.74 (31)	7.70–8.47 (22)			
BTB	9.92 ± 0.37	9.68 ± 0.33	9.54 ± 0.34	9.34 ± 0.37	9.04	10.12	10.07
	9.25–10.8 (33)	9.1–10.16 (23)	8.8–10.58 (31)	8.82–10.11 (22)			
LTB	4.90 ± 0.24	4.73 ± 0.21	4.75 ± 0.19	4.64 ± 0.14	4.47	4.75	4.71
	4.45–5.40 (29)	4.33–5.09 (23)	4.41–5.26 (31)	4.24–4.84 (22)			
WET	1.21 ± 0.12	1.16 ± 0.07	0.99 ± 0.10	0.99 ± 0.09	0.84	1.10	0.88
	1.05–1.44 (25)	0.99–1.31 (18)	0.80–1.23 (30)	0.84–1.22 (21)			
NB	3.58 ± 0.35	3.42 ± 0.22	3.08 ± 0.26	2.85 ± 0.22	2.90	2.98	2.89
	2.96–4.15 (30)	2.95–3.7 (23)	2.38–3.53 (31)	2.45–3.16 (22)			
BRC	4.71 ± 0.27	4.51 ± 0.21	4.49 ± 0.23	4.20 ± 0.20	4.22	4.12	4.46
	4.3–5.50 (30)	4.13–4.89 (23)	3.87–4.82 (31)	3.80–4.59 (22)			
BRJ	8.57 ± 0.43	8.09 ± 0.51	8.69 ± 0.50	7.91 ± 0.40	7.77	8.02	8.29
	7.84–9.30 (30)	7.35–9.15 (23)	7.79–9.73 (31)	7.09–8.86 (22)			
LIB	4.92 ± 0.22	4.77 ± 0.26	4.87 ± 0.22	4.69 ± 0.16	4.62	4.34	4.81
	4.53–5.30 (33)	4.33–5.40 (23)	4.46–5.28 (31)	4.44–5.05 (22)			
POC	5.14 ± 0.24	5.16 ± 0.25	5.29 ± 0.21	5.31 ± 0.17	5.96	4.95	5.39
	4.73–5.60 (33)	4.40–5.55 (23)	4.66–5.67 (31)	5.04–5.62 (22)			
BBC	11.63 ± 0.42	11.27 ± 0.22	11.13 ± 0.40	10.94 ± 0.45	10.33	10.53	11.03
	10.79–12.7 (30)	10.95–11.66 (23)	10.31–11.75 (31)	10.27–11.88 (22)			
ZB	16.40 ± 0.71	15.74 ± 0.84	15.55 ± 0.59	14.68 ± 0.54	–	14.68	15.69
	15.32–17.63 (30)	14.7–17.72 (22)	14.23–16.48 (31)	13.85–15.85 (22)			
LM	20.56 ± 0.76	19.71 ± 0.90	19.31 ± 0.79	18.34 ± 0.60	18.54	19.00	20.05
	19.05–22.09 (33)	17.94–21.54 (22)	16.68–20.41 (31)	17.17–19.66 (22)			
LMS	6.28 ± 0.15	6.27 ± 0.19	5.75 ± 0.19	5.87 ± 0.23	5.70	5.97	6.07
	5.94–6.51 (31)	6.00–6.69 (23)	5.12–6.18 (31)	5.62–6.75 (22)			
Lm4	1.69 ± 0.09	1.74 ± 0.12	1.50 ± 0.04	1.51 ± 0.05	1.42	1.54	1.50
	1.54–1.90 (32)	1.55–2.00 (23)	1.35–1.58 (31)	1.39–1.62 (22)			
Wm2	0.98 ± 0.10	1.01 ± 0.10	0.87 ± 0.06	0.85 ± 0.05	0.82	0.93	0.90
	0.83–1.20 (32)	0.77–1.16 (23)	0.76–0.98 (31)	0.72–0.92 (22)			

Measurements are given as: mean ± standard deviation; min–max (sample size). For descriptions of measurements, see the Measurements section.

*Holotype (BMNH 27.11.1.268) of *Marmosa agilis peruana* (age class 6).

†Holotype (BMNH 11.4.25.24) of *Marmosa beatrix* (age class 6).

‡Holotype (BMNH 26.12.4.91) of *Marmosa agilis buenavistae* (age class 8).

Table 5. Results of Student's *t*-tests for sexual dimorphism in *Gracilinanus agilis* and *Gracilinanus peruanus*, and between the species for males and females separately

	Gracilinanus agilis		*Gracilinanus peruanus*		*G. agilis* × *G. peruanus* Males		*G. agilis* × *G. peruanus* Females	
	t	*P*	*t*	*P*	*t*	*P*	*t*	*P*
GLS	4.533	**0.000**	6.503	**0.000**	5.964	**0.000**	6.351	**0.000**
CBL	5.106	**0.000**	6.473	**0.000**	5.774	**0.000**	6.217	**0.000**
RL	3.484	**0.001**	3.251	**0.002**	5.137	**0.000**	3.961	**0.000**
NL	3.166	**0.003**	4.371	**0.000**	4.960	**0.000**	4.692	**0.000**
PL	2.987	**0.004**	5.033	**0.000**	3.012	**0.004**	4.649	**0.000**
MTR	0.586	0.561	6.310	**0.000**	3.444	**0.001**	8.185	**0.000**
UMS	1.187	0.240	0.125	0.901	10.957	**0.000**	8.204	**0.000**
LM4	1.182	0.243	1.213	0.231	6.912	**0.000**	5.618	**0.000**
WM2	0.806	0.424	0.165	0.869	6.287	**0.000**	3.349	**0.002**
HC	3.794	**0.000**	4.667	**0.000**	−0.759	0.451	00.276	0.784
PB	2.104	**0.040**	1.847	0.071	9.893	**0.000**	8.569	**0.000**
BTB	2.383	0.021	2.126	0.038	4.160	**0.000**	3.332	**0.002**
LTB	2.647	0.011	2.502	0.016	2.608	0.012	1.767	0.084
WET	1.420	0.163	0.177	0.861	7.513	**0.000**	6.579	**0.000**
NB	1.891	0.064	3.295	**0.002**	6.355	**0.000**	8.785	**0.000**
BRC	2.970	0.005	4.782	**0.000**	3.511	**0.001**	5.090	**0.000**
BRJ	3.740	**0.000**	6.075	**0.000**	−0.990	0.326	1.282	0.207
LIB	2.239	0.029	3.088	**0.003**	0.927	0.358	1.238	0.223
POC	−0.249	0.804	−0.454	0.652	−2.535	0.014	−2.370	0.022
BBC	3.775	**0.000**	1.588	0.118	4.866	**0.000**	3.135	**0.003**
ZB	3.073	**0.003**	5.493	**0.000**	5.082	**0.000**	4.954	**0.000**
LM	3.791	**0.000**	4.855	**0.000**	6.461	**0.000**	5.964	**0.000**
LMS	0.280	0.780	−2.114	0.039	12.106	**0.000**	6.313	**0.000**
Lm4	−1.514	0.136	−0.667	0.508	10.320	**0.000**	8.207	**0.000**
Wm2	−1.012	0.316	1.149	0.256	5.418	**0.000**	6.458	**0.000**

In bold, significant values with $P < 0.05$. For measurement descriptions, see the Measurements section.

Table 6. Percentage of variance explained by the first three components of the principal component analysis (PCA)

Principal component	% of variance	Cumulative %
1	50.242	50.242
2	18.424	68.666
3	5.485	74.151

In the PCA, the first component corresponded to 50.2% of the total variance and the second component corresponded to 18.4% (Table 6). Except for pos-orbital constriction (POC), all coefficients had positive values in the first component, indicating that this component is related to the general size of the skull. The nasal breadth (NB) was the dimension that mostly contributed to the first component variance followed by the width of the ectotympanic (WET), length of M4 (LM4), width of m2 (Wm2), and length of m4 (Lm4) (Table 7). By plotting the coefficients of the first and second principal components, specimens that were previously identified as *G. agilis* or *G. peruanus* (based on qualitative external and craniodental diagnostic traits) exhibited narrow morphometric overlap in the plane of the first two principal components (Fig. 3). The specimens concentrated in the left portion of Figure 3 were identified as *G. peruanus*, including the holotypes of *Marmosa agilis buenavistae* and *M. a. peruana*. The specimens in the right portion correspond to *G. agilis*. The holotype of *M. beatrix*, identified in this study as part of the *G. agilis* species complex, is located in the lower part of the scatter plot, on the border of the morphometric range of *G. agilis* (Fig. 3).

In the discriminant analysis, the first function corresponded to 86.6% of the total variance and the second function corresponded to 10.4% (Table 8). The variable that mostly contributed to discriminate *G. agilis*, *G. peruanus*, and the holotypes of *Marmosa agilis peruana*, *M. a. buenavistae*, and *M. beatrix* in the first discriminant function was CBL, followed by BRJ, PB, LM, and GLS, all of which were related to either the length of the skull or the width of the rostrum

Table 7. Coefficients of the first three components of the principal component analysis (PCA)

	Component		
Variable	1	2	3
GLS	0.017	0.009	0.004
CBL	0.019	0.011	0.005
RL	0.023	0.010	0.003
NL	0.024	0.009	0.003
PL	0.014	0.011	0.006
MTR	0.013	0.004	0.001
UMS	0.013	-0.002	-0.002
LM4	**0.039**	**-0.013**	0.004
WM2	0.018	-0.002	-0.004
HC	0.011	**0.051**	**-0.020**
PB	0.022	-0.001	0.004
BTB	0.011	0.002	**0.007**
LTB	0.007	0.008	-0.002
WET	**0.045**	-0.010	**-0.019**
NB	**0.046**	0.001	0.006
BRC	0.021	0.011	**0.008**
BRJ	0.014	**0.016**	**0.016**
LIB	0.010	**0.012**	**0.007**
POC	-0.006	0.000	-0.001
BBC	0.009	0.002	0.005
LM	0.019	0.011	0.003
LMS	0.016	-0.010	-0.004
Lm4	**0.032**	-0.011	-0.004
Wm2	**0.034**	**-0.021**	-0.002

In bold, the five larger values for each component.

(Table 9). When we plotted the coefficients of the first and second discriminant functions, we obtained three well-separated groups (Fig. 4). The specimens on the upper left portion of the figure represent *G. peruanus*, as well as the holotypes of *Marmosa agilis buenavistae*, and *M. a. peruana*, the specimens in the upper right portion of the figure correspond to *G. agilis*, and at the bottom of the figure lies the holotype of *M. beatrix* as a separate morphometric group from both *G. peruanus* and *G. agilis* (Fig. 4).

Although *G. agilis* and *G. peruanus* showed a narrow morphometric overlap in the bivariate plot of the first and second principal components in PCA (Fig. 3), in the DA these species were very distinctive in morphometric space (Fig. 4). Most specimens of *G. agilis* were placed on the right side of the PCA bivariate plot and did not overlap with specimens of *G. peruanus* along the first principal component axis, showing that they differ in general size (Fig. 3). Regarding DA, the species were completely separated in the bivariate plot of the first and second discriminant functions (Fig. 4), with dimensions related to the skull length (GLS, CBL, and LM) and rostral width (PB and BRJ) being the most important variables segregating these species.

SUMMARY

Our morphological and molecular data showed the existence of remarkable differences among specimens of *G. agilis* from Mato Grosso and Rondônia states compared with other populations of central–western Brazil. Geographically structured patterns of external and craniodental morphology, together with high levels of genetic divergence (Cyt*b* sequences) between two reciprocally monophyletic groups herein recovered, and the discovery of two localities with morphologically distinct specimens occurring in sympatry, indicated a species complex within *G. agilis*. Finally, the analysis of the type material of the nominal taxa currently associated with *G. agilis* led us to treat *Marmosa agilis peruana* Tate, 1931 as a valid species, resurrecting this name from the synonym of *G. agilis*, herein spelled as *Gracilinanus peruanus*.

TAXONOMY

GRACILINANUS PERUANUS (TATE, 1931)

Synonyms (first usage of each synonym only)

Marmosa marica: Thomas, 1927: 608; part (includes specimens from Tingo Maria, Peru).

Marmosa agilis buenavistae Tate, 1931: 10; type locality 'Buenavista, Department of Santa Cruz, Bolivia'.

Marmosa agilis peruana Tate, 1931: 11; type locality 'Tingo Maria, Rio Huallaga, Peru, 2000 feet'.

Marmosa agils peruania: Tate, 1933: legend of plate 11; incorrect subsequent spelling of *Marmosa agilis peruana* Tate.

Thylamys rondoni Miranda-Ribeiro, 1936: 387; part (includes one specimen of the type series from São João da Serra do Norte, Rondônia).

Marmosa rondoni: Vieira, 1955: 352; new name combination; part (based on the type series of Miranda-Ribeiro, 1936).

Marmosa [(*Thylamys*)] *agilis buenavistae*: Cabrera, 1958: 28; new name combination.

Marmosa [(*Thylamys*)] *agilis peruana*: Cabrera, 1958: 28; new name combination.

Gracilinanus agilis: Gardner & Creighton, 1989: 5; new name combination; part (*buenavistae* and *peruana* in synonymy).

Gracilinanus agilis buenavistae: Anderson, 1993: 18 (general distribution records).

Gracilinanus agilis buenavista: Langguth, Limeira and Franco, 1997: 7; incorrect subsequent spelling of *Marmosa agilis buenavistae* Tate; part (based on the type series of Miranda-Ribeiro, 1936).

Type information

BMNH 27.11.1.268, collected on 20 January 1927 by R.W. Hendee. The holotype is an adult male (age class 6).

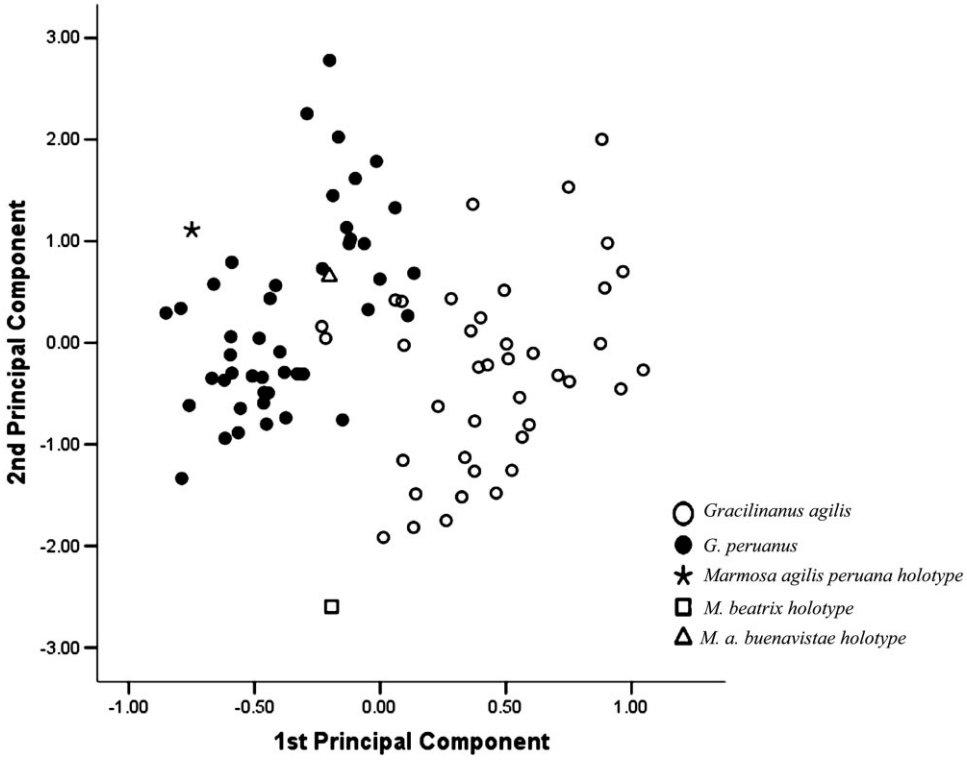

Figure 3. Scatter plot of the principal component analysis (PCA) of 24 log-transformed craniodental measurements of *Gracilinanus agilis*, *Gracilinanus peruanus*, and other nominal taxa related to these species.

Table 8. Eingenvalues from the discriminant analysis (DA)

Function	Eingenvalue	% of variance	cumulative %
1	12.160	86.6	86.6
2	1.460	10.4	97.0
3	0.427	3.0	100.0

Although the type is a skin and skull in good condition, the right zygomatic arch is broken and the palate is partially broken and unclean, making it difficult to visualize the palatine fenestrae.

Type locality

'Tingo Maria, Rio Huallaga', Huánuco, Peru – (09°08′S, 75°57′W–600 m., Hershkovitz, 1992).

Geographic distribution

The collecting localities of *G. peruanus* comprise central Peru, central Bolivia, and western Brazil, in the states of Rondônia and north-western Mato Grosso. By connecting the most external collecting localities of the species we obtained an approximated geographic distribution that extends from central Peru to central Bolivia and western Brazil, in the northern and central portions of Mato Grosso state (Fig. 1). This area presents two records where *G. peruanus* and *G. agilis* occur in sympatry (localities 3 and 15; Fig. 1).

Emended diagnosis

Gracilinanus peruanus is a small-sized didelphid marsupial that differs from other congeners by the following combination of morphological characters (see Table 10): dorsal pelage dull reddish brown; grey-based ventral pelage from chest to anus; usually poorly developed circumocular mask; head and body length 85.0–121.0 mm; tail length 130.0–155.0 mm; greatest length of skull 24.50–28.91 mm (Table 4); interorbital region usually smooth, sometimes with angular supraorbital margins of the frontals (i.e. margins with sharpened edges, not described by Voss & Jansa, 2003, 2009), never showing incipient postorbital processes; relative position of maxillary fenestra aligned anteriorly with the paracone of P3 and posteriorly with the paracone of M1 or M2; posterolateral palatal foramen usually smaller than palatine fenestra; second foramen ovale present, usually formed by a wide bony strut on the anteromedial region of the alisphenoid tympanic process; paraoccipital process usually very small and rounded; mastoid process usually incipient or absent; and upper canine usually with a posterior accessory cusp, rarely with a small anterior accessory cusp (Figs 5–10).

Table 9. Coefficients of the first three functions of the discriminant analysis (DA)

	Function		
Variable	1	2	3
GLS	**0.646**	0.241	**–1.350**
CBL	**–1.323**	0.188	**–0.845**
RL	0.234	**0.632**	0.224
NL	–0.046	–0.617	–0.031
PL	–0.405	–0.314	0.045
MTR	–0.004	0.145	0.190
UMS	0.238	0.285	–0.553
LM4	0.060	–0.299	**0.847**
WM2	–0.031	0.076	0.337
HC	0.055	0.600	**0.708**
PB	**0.735**	0.417	0.503
BTB	–0.030	**–0.864**	0.252
LTB	0.228	–0.108	–0.004
WET	0.225	–0.175	–0.590
NB	0.362	0.340	–0.008
BRC	0.174	0.512	0.534
BRJ	**–0.839**	**–0.682**	–0.598
LIB	–0.230	0.105	–0.370
POC	–0.415	0.118	0.344
BBC	0.193	**0.746**	–0.137
LM	**0.685**	**–0.697**	**1.560**
LMS	0.028	0.113	0.346
Lm4	0.420	0.236	–0.240
Wm2	0.019	–0.077	0.067

In bold, the five larger values for each function.

Description

Gracilinanus peruanus is a small-sized marsupial (Table 4) with short (approximately 7 mm in length), smooth, and dull reddish-brown dorsal pelage, not exposing the grey-based hairs (Fig. 5); pelage of rostrum short with grey-based and cream-tipped hairs, usually contrasting sharply with darker crown fur that is longer and grey-based with reddish-tipped hairs; dark circumocular mask small and poorly developed anteroposteriorly when compared with other *Gracilinanus* species (Fig. 10); colour pelage between eyes and ears usually reddish, similar to the colour of head; cheeks self-coloured cream contrasting sharply with facial mask; mystacial vibrissae entirely black or black with white tips; three or four black genal vibrissae dorsally oriented and three genal white vibrissae ventrally oriented; white submental and interamal vibrissae present; the self-coloured cream portion of ventral pelage extends from chin to chest and forearms, and grey-based hairs extend from chest to inguinal region, including hind limbs; tail slightly bicoloured, longer than combined length of head and body; fur of the base of the tail no longer than 5 mm in length; caudal scales arranged in annular pattern; each scale possesses three hairs inserted in its posterior margin, with the central hair slightly longer (two caudal scales in length); hairs on the basal portion of the tail shorter and more sparse, giving the ventral and distal portion of the tail a more hairy aspect; prehensile ventral surface of the distal part of the tail approximately 30 mm in length; ears small (14–19 mm), cream to cream–orange on the base and pale brown distally.

Craniodentally, premaxillary rostral process present; nasals long, extending anteriorly beyond I1; rostrum short and wide; two lacrimal foramina present on each side of the skull, both not visible in dorsal or lateral views; interorbital region with parallel margins; supraorbital margins vary from smoothly rounded (young specimens) to slightly angular (adult specimens); postorbital processes absent (Fig. 7); petrosal laterally exposed through a fenestra in the parietal–squamosal suture; incisive foramen small, reaching the posterior edge of canines; maxillo-palatine fenestrae present; maxillary fenestrae present, with anterior margin aligned with the paracone of P3 and the posterior margin aligned with the paracone of M1, metacone of M1, or the paracone of M2; palatine fenestrae present; posterolateral palatal foramen usually smaller than palatine fenestra (Fig. 8); paraoccipital process very small and rounded; mastoid process usually incipient or absent; alisphenoid tympanic process globular; second foramen ovale present, usually formed by a wide bony strut on the anteromedial region of the alisphenoid tympanic process (Fig. 9); I1 longer than I2–I5; I2–I5 similar in size; upper canine short, usually with posterior accessory cusps and rarely with small anterior accessory cusps; P1 smaller than P2 and P3; P2 either taller or subequal in height than P3 (Fig. 8).

Comparisons with congeners

Gracilinanus peruanus differs from other congeneric species by exhibiting dull reddish brown dorsal fur versus the reddish, brownish, or greyish tones in other species (see Table 10); grey-based buffy ventral fur from chest to anus, as in *G. agilis* and *G. marica* versus self-white in *G. emiliae* and with grey-based hairs from throat to anus in *G. aceramarcae*, *G. dryas*, and *G. microtarsus*; circumocular mask restricted to the area close to the eyes, similar to *G. agilis* but differing from the other species in which the masks are wider (Fig. 10); posterior accessory cusps in upper canines frequently present versus absent in *G. aceramarcae*, *G. agilis*, and *G. microtarsus*; interorbital region smooth or with angular supraorbital margins in mature adults versus weakly and distinctly beaded in *G. marica* and *G. emiliae*, respectively; and well-developed maxillary fenestrae, which are small or absent in *G. emiliae*.

A summary of the diagnostic characters of *G. peruanus* in comparison with the other species of the genus is provided in Table 10. Closer comparisons between *G. agilis* and *G. peruanus* are warranted, as the latter

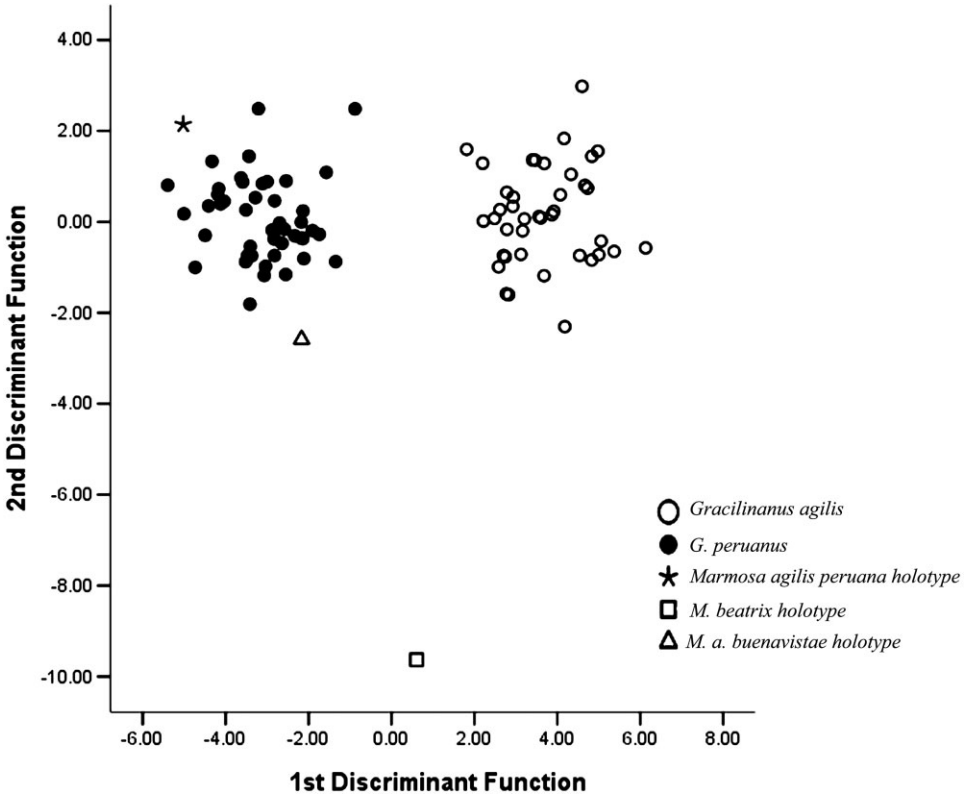

Figure 4. Scatter plot of canonical scores (DA) for discriminant functions 1 and 2 based on craniodental measurements of *Gracilinanus agilis*, *Gracilinanus peruanus*, and other nominal taxa related to these species.

was until now considered a junior synonym of the former, and both species are present in Bolivia and central–western Brazil, including two sympatric records (Fig. 1). In fact, *G. peruanus* and *G. agilis* are very similar in external and craniodental traits; however, the former exhibits dull reddish brown dorsal fur whereas the latter exhibits dorsal fur with brownish/greyish tones (Fig. 5). In addition, *G. peruanus* is generally smaller in size when compared with *G. agilis* (Table 4).

Craniodentally, the most distinctive character that distinguishes these species is the relative position of the anterior margin of the maxillary fenestrae, which is consistently aligned with the paracone of P3 in *G. peruanus* versus consistently aligned with the paracone of M1 in *G. agilis* (Fig. 8). It is important to mention, however, that in young specimens of *G. peruanus* the position of the maxillary fenestrae is similar to the position found in specimens of *G. agilis*.

Although we found intraspecific variation in the craniodental traits analysed herein, we found remarkable differences in the frequencies in which they appear in each species (Table 11). In this sense, these species differ in relation to the posterior accessory cusps in the upper canines, which is frequently present in *G. peruanus*, but usually absent in *G. agilis*; in the relative size of posterolateral palatal foramen when compared with the palatine fenestra, which is usually smaller in *G. peruanus* and usually larger in *G. agilis*; and in the morphology of the alisphenoid tympanic process, as it generally exhibits a wide bony strut in *G. peruanus* versus a narrow bony strut in *G. agilis* (Fig. 9; Table 11). The interorbital region appears to be somewhat different between these species. Both species generally exhibit a smooth interorbital region in younger specimens, but with slightly angular margins in older specimens. This latter condition appears to be more developed in *G. agilis*, in which even an incipient postorbital process may be present (versus absent in *G. peruanus*; Fig. 7). There are also differences related to the projection of the paraoccipital and mastoid processes (of petrosal), which are more developed in *G. agilis* than in *G. peruanus* (Fig. 9). The paraoccipital process is often large and squared in appearance in *G. agilis*, whereas it is smaller and rounded in appearance in *G. peruanus*. The mastoid process is much more developed in *G. agilis*, whereas in *G. peruanus* it is incipient or absent (Fig. 9).

Intraspecific morphological variation

We observed few pelage variations in examined specimens of *G. peruanus*. The dorsal pelage followed the

Table 10. Comparisons between the six valid species of *Gracilinanus* and *Gracilinanus peruanus* based on selected morphological traits

	Gracilinanus aceramarcae	*Gracilinanus agilis*	*Gracilinanus dryas*	*Gracilinanus emiliae*	*Gracilinanus marica*	*Gracilinanus microtarsus*	*Gracilinanus peruanus*
Adult LT/HBL ratios	1.50–1.52 (n = 3)[a]	1.08–1.63 (n = 60)	1.20–1.68 (n = 6)[a]	1.64–1.96 (n = 4)[a]	1.32–1.38 (n = 5)[a]	1.38–1.66 (n = 7)	1.16–1.64 (n = 33)
Dorsal pelage[b]	Reddish brown, long pelage	Brown to greyish brown, short pelage	Dark reddish-brown, long pelage	Warm reddish brown, rather long pelage[c]	Brown to reddish brown, long pelage, wavy in appearance	Brown to chestnut brown, long pelage	Dull reddish brown, short pelage
Ventral pelage	Grey based with orange tips, except chin self-coloured light orange	Grey based with cream or yellow tips except chin, throat and chest self-coloured cream or yellow[d]	Grey based with reddish brown tips except chin self-coloured light reddish brown	Entirely self-white or cream	Grey based with cream tips, except chin, throat and chest self-coloured cream	Grey based with cream or yellow tips, except chin self-coloured cream or yellow	Grey based with white or cream tips, except chin, throat and chest self-coloured cream
Circumocular mask	Developed	Developed to poorly developed	Developed	Developed	Developed	Developed to highly developed	Usually poorly developed
Interorbital region	Smoothly rounded with quite posteriorly divergent margins (beads or processes absent)	Smoothly rounded with parallel margins or incipient postorbital processes; angular margins in mature specimens	Smoothly rounded with quite posteriorly divergent margins (beads or processes absent)	Supraorbital margins distinctly beaded and parallel	Supraorbital margins weakly beaded and parallel	Smoothly rounded with parallel margins or incipient postorbital processes (never beaded)	Smoothly rounded with parallel margins; angular margins in mature specimens[e]
Accessory cusps in upper canine	Absent	Usually absent	Usually present	Present	Usually present	Absent	Usually present[f]
Maxillary fenestrae (palate position)[g]	Developed (between M1/M2)	Developed (between M1/M2, rarely M1/M3)	Developed (between P3/M2)	Absent or small (between M1/M1)	Developed (between P3/M2)	Developed (between P3/M2)	Developed (between P3/M1 or M2)
Posterolateral palatal foramen relative to the palatine fenestra	Larger	Usually larger[f]	Smaller	Smaller	Larger	Smaller	Usually smaller[f]
Morphology of the alisphenoid tympanic process	With wide bony strut	Usually with narrow bony strut[f]	With wide bony strut	With wide bony strut	With wide bony strut	With narrow bony strut	Usually with median or wide bony strut[f]
Upper molar length (in mm)	5.1–5.6 (n = 5)[h]	5.2–5.9 (n = 62)	5.4–5.8 (n = 10) [h]	4.8–5.1 (n = 5)[h]	5.3–5.6 (n = 7)[h]	5.4–5.9 (n = 8)	4.9–5.5 (n = 41)

[a]Extracted from Voss *et al*. (2009). The holotype of *Gracilinanus aceramarcae* (AMNH 72568) exhibits a ratio of 1.35; the holotype of *Gracilinanus marica* (BMNH 98.5.15.1) exhibits a ratio of 1.30.
[b]Reddish forms pass through a gradient of red, from a darker coloration (almost red wine) in *G. dryas*, red in *G. aceramarcae*, lighter red in *G. peruanus*, to a bright red (almost orange) in *G. emiliae*, and a light red mixed with brown in *G. marica*. Brownish forms includes *G. microtarsus*, washed with reddish tones, and *G. agilis*, presenting a lighter brown coloration mixed with greyish hairs.
[c]Tate (1933) refers to a rather short pelage; examination of the holotype (BMNH 9.3.9.10) and other specimens showed longer pelage (around 8 mm) than in *G. agilis* (around 6 mm) and *G. peruanus* (around 7 mm), but shorter than in *G. aceramarcae* (around 12 mm), *G. dryas* (around 12 mm), *G. marica* (around 10 mm), and *G. microtarsus* (around 10 mm).
[d]The holotype of *Marmosa beatrix* exhibits venter entirely self-coloured cream.
[e]The topotype of *Marmosa agilis peruana* (BMNH 27.11.1.269) exhibits wide and divergent supraorbital margins, probably because of the fact that it is a subadult specimen, age class 5.
[f]We found variation in this character for this species (see text and Table 11).
[g]The relative maximum length of the fenestrae are in parentheses: for example, P3/M2, from about paracone of P3 to about paracone of M2.
[h]Extracted from Voss *et al*. (2009).

Figure 5. Dorsal view of skin. Left to right: *Gracilinanus peruanus* (UFMT 872, locality 1 in Fig. 1, female, age class 7) and *Gracilinanus agilis* (UFMT 1039, locality 36 in Fig. 1, male, age class 8). Scale bar: 10 mm.

same pattern in all examined material, except for a few specimens that exhibited a less homogeneous pelage; however, more expressive variation was observed in the ventral pelage, with several specimens (CM 455, 463, 464, 489, 492, locality 3; Fig. 1) exhibiting self-coloured cream pelage in the inguinal region, and other specimens (UFMT 3816, locality 23; AMNH 209157, locality Costa Marques, Rondônia, not shown in Fig. 1) exhibiting self-coloured cream pelage over the entire venter. In most specimens, however, self-coloured fur is restricted to the chin, throat, chest, and frontal limbs. Intraspecific variation observed in the presence of C1 accessory cusps, the size of posterolateral palatal foramen, and the morphology of the anteromedial process of the alisphenoid tympanic process are shown in Table 11.

Figure 6. Dorsal, ventral, and lateral views of the skull and lateral view of the mandible of *Gracilinanus peruanus* (UFMT 1333, locality 2 in Fig. 1, female, age class 7). Scale bar: 5 mm.

Taxonomic comments

The combination of diagnostic morphological characters mentioned in the Emended diagnosis section, together with the results of the morphometric and molecular analyses, justify the recognition of a distinct species of gracile mouse opossum. To search for available names that could be assigned to this distinct species we have examined the holotypes of nominal taxa related to *G. agilis*, such as *beatrix* Thomas, 1910; *buenavistae* Tate, 1931; *peruana* Tate, 1931; *blaseri* Miranda-Ribeiro, 1936; and *rondoni* Miranda-Ribeiro, 1936 (Voss *et al*., 2005: table 1).

Regarding the holotype of *M. beatrix* (BMNH 11.4.23.24), it can be consistently associated with the genus *Gracilinanus* by the presence of maxillary fenestrae, an anteromedial process of the alisphenoid tympanic process, and P2 taller than P3. Nevertheless, the taxonomic status of this nominal taxon requires further evaluation because the holotype exhibits self-coloured cream pelage covering the entire venter, and is smaller in the majority of the craniodental measurements, differing in the ventral coloration and

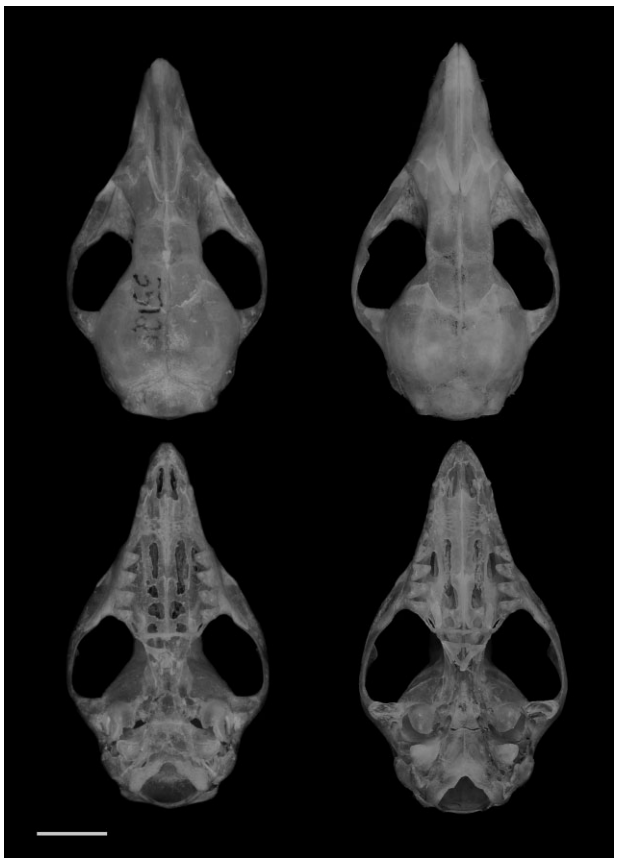

Figure 7. Dorsal and ventral views of the skull of *Gracilinanus peruanus* (MZUSP 35121, locality 2 in Fig. 1) and *Gracilinanus agilis* (MZUSP 35286, locality 43 in Fig. 1). Both specimens are male individuals of age class 7. Scale bar: 5 mm.

size of typical *G. agilis* (Table 4). In addition, the multivariate analyses showed that this specimen does not group with either *G. agilis* or *G. peruanus* in morphometric space (Figs 3, 4).

Miranda-Ribeiro (1936) described two species that are currently in the synonym of *G. agilis*: *M. blaseri*, based on a specimen from São Bento, Goiás (MN 1250) and *T. rondoni*, based on a type series from two distinct localities: Salto do Sepotuba, Mato Grosso state (MN 1270) and São João da Serra do Norte, Rondônia state (MN 1271, 1272, 1275, and 1276). The holotype of *M. blaseri* can be assigned to *G. agilis* based on its greyish brown dorsal coloration, absence of cusps in the C1, relative position of maxillary fenestra between M1 and M2, and a posterolateral palatal foramen larger than the palatine fenestra.

In relation to *T. rondoni*, the type series is a composite. Miranda-Ribeiro (1955) designated the specimen MN 1270 from Salto do Sepotuba, Mato Grosso, as the lectotype, and the other material, consequently, as paralectotypes (see also Langguth *et al*., 1997). Among the latter specimens, MN 1276 can be consistently assigned to *G. peruanus* based on its dull reddish brown dorsal coloration, maxillary fenestra between P3 and M2, a posterolateral palatal foramen smaller than the palatine fenestra, and the presence of a second foramen ovale formed by a wide bony strut on the anteromedial region of the alisphenoid tympanic process. The remaining paralectotypes do not belong to the genus *Gracilinanus* nor the lectotype.

By contrast, the specimens herein identified as a distinct species of gracile mouse opossum are morphometrically and morphologically similar to the holotypes of *M. a. buenavistae* Tate, 1931 (BMNH 26.12.4.91) and *M. a. peruana* Tate, 1931 (BMNH 27.11.1.268). All of the specimens exhibit dull reddish brown dorsal pelage; posterolateral palatal foramen smaller than palatine fenestra; second foramen ovale formed by a wide bony strut on the anteromedial region of the alisphenoid tympanic process; paraoccipital process small and rounded; and incipient mastoid process. Several minor differences observed between the holotype of *M. a. buenavistae* and our specimens, such as the relatively larger size, the faded greyish brown dorsal pelage coloration, the presence of an incipient postorbital process, and the absence of accessory cusps in the upper canines in the former, can be related to age variation because the specimen is a mature adult female (age class 8). Other morphological traits, such as the anterior margin of the maxillary fenestrae that only slightly reaches the posterior border of P3 in both holotypes, and the absence of accessory cusps in C1 in the holotype of *M. a. peruana*, are within the scope of morphological variation observed in the specimens in central–western Brazil and the surrounding areas; however, among all the specimens examined, only the holotype and a topotype of *M. a. peruana* (BMNH 27.11.1.268–269) exhibited developed circumocular masks. In the absence of other specimens from Peru and nearby vicinities, we provisionally treat this difference as a geographical variation in this trait.

Based on these results, we recognize *M. a. buenavistae* Tate, 1931 and *M. a. peruana* Tate, 1931 as synonyms that can be assigned to a valid species distinct from *G. agilis* (Burmeister, 1854). Because both available names were described in the same work by the same author (Tate, 1931) and in the same hierarchical category (as subspecies of *Marmosa agilis*), the priority between these two names cannot be objectively determined. So, as first revisers of this issue, and according to article 24.2 of the International Code of Zoological Nomenclature (ICZN, 1999), we establish *M. a. peruana* Tate, 1931 as the name for the species recognized in this report, with *M. a. buenavistae* Tate, 1931 treated as its junior synonym. We use the spelling of this taxon as *G. peruanus* following the agreement in gender according to article 31.2 of the ICZN (1999).

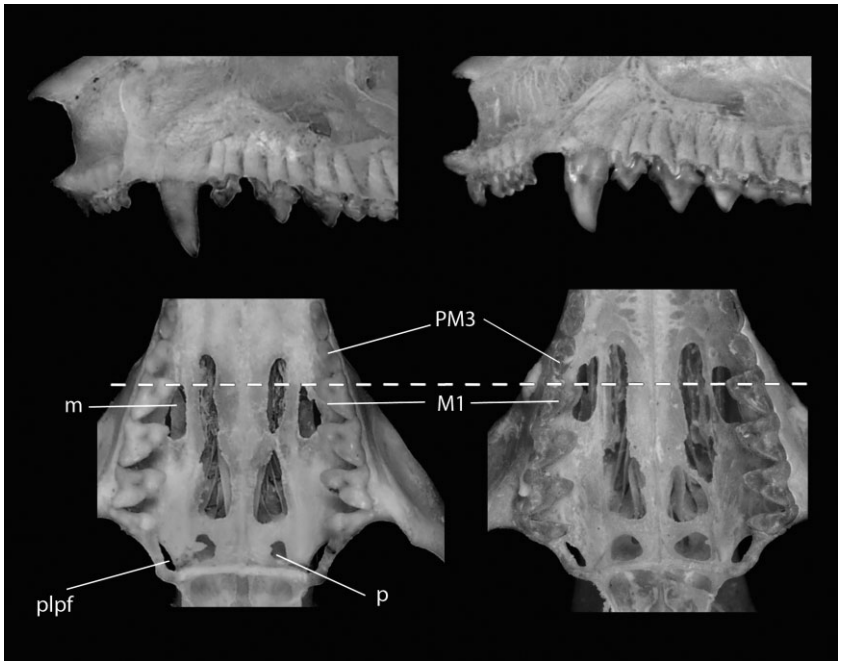

Figure 8. Upper canine morphology with accessory cusps absent in *Gracilinanus agilis*, upper left (MZUSP 35286, locality 43 in Fig. 1, male, age class 7); usually present in *Gracilinanus peruanus*, upper right (UFMT 1333, locality 2 in Fig. 1, female, age class 7). Size differences between posterolateral palatal foramen (plpf) in relation to palatine fenestra (p): smaller in *G. peruanus* (UFMT 3816, locality 23 in Fig. 1, male, age class 7), and larger or similar in size in *G. agilis* (MZUSP 35311, locality 30 in Fig. 1, male, age class 7). Note the position of the maxillary fenestra (m) in *G. agilis* (M1/M2) from the metacone of M1 to the paracone of M2, and in *G. peruanus* (P3/M1 or M2) from the paracone of P3 to the paracone of M2 (see Table 10). Pictures are not shown to scale to better visualize these characters.

Reproductive data

Within our sample, we found five lactating adult females collected in the dry season (August 2006 and October 2007), as demonstrated by the discoloured inguinal region and enlarged nipples, thus giving a completely cream coloration to the inguinal region (UFMT 870, 872, 873, 1333; CM 492); the abdominal–inguinal mammae formula of these specimens is 4-1-4 = 9; however, the female AMNH 209157 has 3-1-3 = 7 (S. Anderson, annotation in the specimen tag).

Regarding sexually dimorphic characters, the adult males belonging to age classes 6 and 7 (*sensu* Rossi *et al*., 2010b) present a knob-like, lateral carpal tubercle (UFMT 876, 3816; CM 455, 457, 464, 489; MZUSP 35121, 35112), whereas a young male (UFMT 1370) belonging to age class 3 has a very small, knob-like lateral carpal tubercle. This structure was absent in all females examined, whereas medial carpal tubercles were absent in both sexes.

Field data

Among specimens of *G. peruanus* with available field information, two were caught in Sherman live traps placed on the ground and 11 were caught in pitfall traps. Although pitfall traps appear to be more effective in collecting the species, it is not possible to confirm this because we have no information about the trapping efforts. Considering the distinct ecoregions (*sensu* Olson *et al*., 2001) within the geographic range of *G. peruanus*, 12 of our records are located in the Chiquitano dry forests (including the holotype of *M. a. buenavistae*, locality 67; Fig. 1), followed by 11 records in the Cerrado, two records in the Madeira-Tapajós moist forests, one record in the Mato Grosso seasonal forests, and one record in the Ucayali moist forests (the holotype of *M. a. peruana*, locality 71, Fig. 1). For most collecting localities in the Cerrado and for a few localities in the Chiquitano dry forests, the specimens are associated with gallery forests such as those shown in Figure 11. In the Cerrado, 20 individuals were collected in gallery and deciduous forests, and seven individuals were collected in both disturbed forests and Cerrado *sensu stricto*. This pattern leads us to consider that this species is associated with forested formations, and may use the gallery forests to enter savanna-like formations in the Brazilian Cerrado.

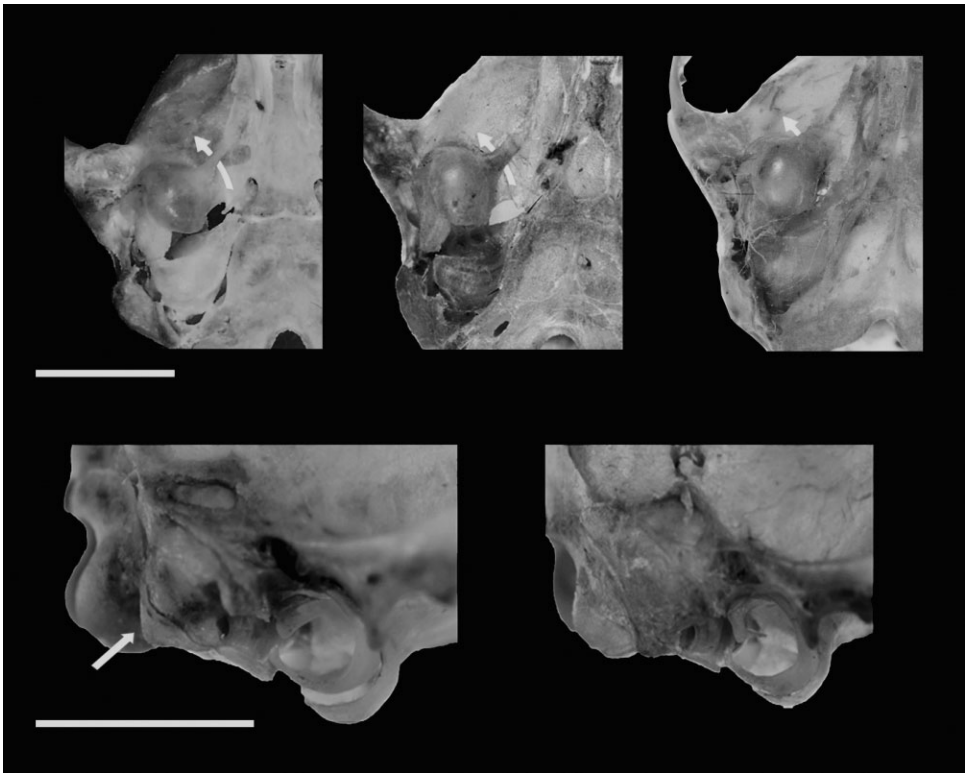

Figure 9. Distinct morphologies of the anteromedial surface of the alisphenoid tympanic process (top) and the paraoccipital and mastoid processes (bottom) in *Gracilinanus*. Upper left: narrow alisphenoid tympanic process, MZUSP 35311, *Gracilinanus agilis* (locality 30 in Fig. 1). Upper central: median alisphenoid tympanic process, MZUSP 35121, *Gracilinanus peruanus* (locality 12 in Fig. 1). Upper right: wide alisphenoid tympanic process, MZUSP 35117, *Gracilinanus peruanus* (locality 10 in Fig. 1). The arrows show the pathway of the mandibular branch of the trigeminal nerve (V^3) through the secondary foramen ovale. Note that the portion of the arrow concealed by the alisphenoid process is notably smaller in MZUSP 35311, whereas it is partially and almost fully enclosed by the alisphenoid tympanic process in MZUSP 35121 and MZUSP 35117, respectively. It is important to note that the condition found in MZUSP 35117 does not correspond to the alisphenoid lamina of Voss & Jansa (2009: fig. 16C), because the latter refers to a posteromedial wide alisphenoid bony strut on the bullar surface that does not span the transverse canal, whereas MZUSP 35117 exhibits a wider alisphenoid bony strut anteromedially positioned on the bullar surface that spans the transverse canal. Lower right: paraoccipital and mastoid processes (of petrosal) often large and squared in appearance in *G. agilis* (UFMT 1039, locality 36 in Fig. 1). Lower left: paraoccipital and mastoid processes (of petrosal) small and rounded in *G. peruanus* (MZUSP 35121, locality 12 in Fig. 1). Scale bar: 5 mm.

Morphological variation within *Gracilinanus agilis* from central–western Brazil

In the examined specimens of *G. agilis*, we found considerable variation in the dorsal pelage coloration, which appears to be geographically related. In fact, we were able to observe three distinct patterns: specimens from eastern Mato Grosso state (localities 34, 35, 36, 37; Fig. 1) are distinguishable from other specimens by exhibiting dull greyish brown dorsal pelage that is smooth in texture, whereas specimens from the Pantanal biome in southern Mato Grosso (localities 28, 29, 31, 32, 46; Fig. 1) exhibit distinctly bright brown dorsal pelage that is also smooth in texture. Finally, three individuals (CM 485, 486, 487) from central Mato Grosso (locality 3, Fig. 1) show a browner tone (somewhat reddish) and somewhat coarser pelage. Specimens from central Mato Grosso, which occur in sympatry with *G. peruanus*, exhibit dorsal pelage very similar to that of *G. peruanus*; side-by-side comparisons clearly reveal that *G. agilis* are not as distinctly reddish in colour as *G. peruanus*, in addition to the cranial evidence distinguishing these specimens.

We also found two different patterns of facial coloration (Fig. 10B,C). Specimens from eastern Mato Grosso exhibit grey pelage coloration between the dark circumocular mask and the base of the ear, sharply contrasting with the cheeks. They also present a well-developed circumocular mask extending posteriorly to the base of the ear (Fig. 10C). By contrast, most

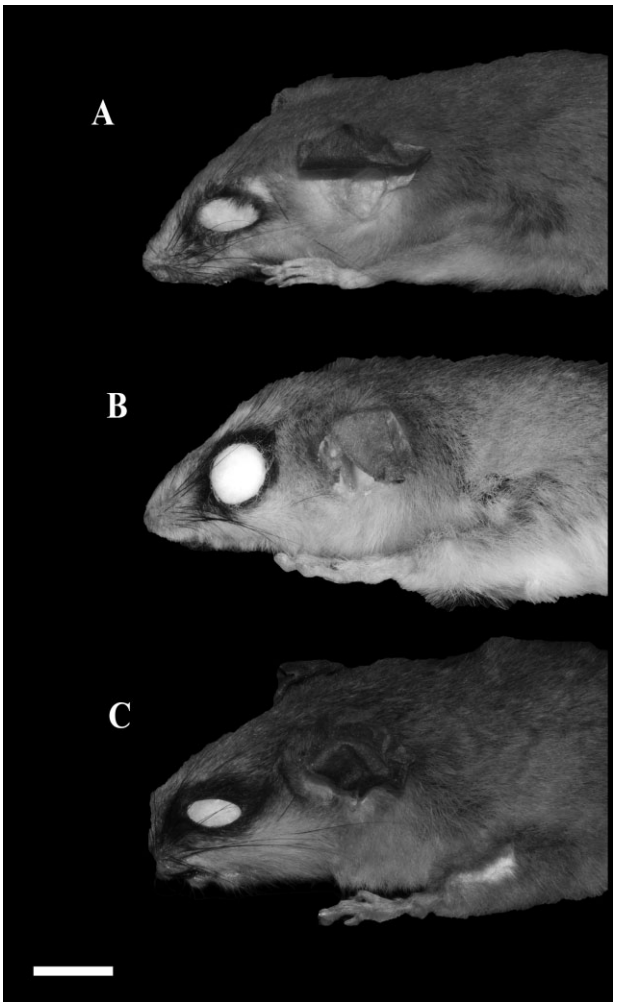

Figure 10. Distinct patterns of the circumocular mask in *Gracilinanus*. A, UFMT 872, *Gracilinanus peruanus*, female, age class 7 (locality 1 in Fig. 1). B, UFMT 692, *Gracilinanus agilis*, male, age class 7 (locality 29 in Fig. 1). C, UFMT 1039, *Gracilinanus agilis*, male, age class 8 (locality 36 in Fig. 1). Scale bar: 10 mm.

specimens from the Pantanal biome exhibit yellowish pelage coloration between the circumocular mask and the base of the ear, and a less developed circumocular mask, similar to *G. peruanus*; however, the pelage between the circumocular mask and the base of the ear is reddish in *G. peruanus* (see Fig. 10; Table 12).

Finally, we found considerable individual variation in the craniodental morphology in *G. agilis*. As seen in Table 11, 95% (n = 65) of the specimens examined herein exhibited no accessory cusps in C1. Moreover, 58% (n = 29) exhibited posterolateral palatal foramen larger than the palatine fenestra, whereas 21% (n = 11) exhibited either smaller or similar posterolateral palatal foramen in relation to the size of the palatine fenestra. Finally, 91% (n = 57) exhibited a narrow anteromedial process of the alisphenoid tympanic process, whereas in the remaining specimens this structure was intermediate in breadth (median in Table 11).

DISCUSSION

The phylogenetic analysis recovered *Gracilinanus* as a monophyletic group with high support, corroborating previous analyses that also used Cyt*b* molecular data (Costa *et al*., 2003; Lóss *et al*., 2011), or that used both mitochondrial and nuclear molecular markers (Voss *et al*., 2009; Faria *et al*., 2013). In this study, the monophyly of the species was also supported in all analyses; however, the partial Cyt*b* was limited in its ability to recover interspecific phylogenetic relationships, as shown by incongruent topologies resulting from different phylogenetic reconstruction methods. All three phylogenetic reconstruction methods agree on the placement of *G. emiliae* as the sister taxon to all other species of *Gracilinanus*. This result is also in agreement with the analysis of Voss *et al*. (2009: fig. 3).

Furthermore, the genetic mean divergence between these clades was comparatively high (12.9–18.2%). The mean genetic distances for Cyt*b* sequences reported in the literature among species of *Gracilinanus* were approximately 15% (Costa *et al*., 2003; Lóss *et al*., 2011), and minimum and maximum values of 13.0 and 20.4%, respectively, were found by Faria *et al*. (2013), which are similar to the values obtained in the present study. The lack of phylogenetic resolution among the other species of *Gracilinanus* prevents us from discussing the relationships within the genus, including the phylogenetic position of *G. peruanus*; however, independent of the true phylogenetic position of *G. peruanus*, it is clear that it is both genetically and morphologically differentiated from all other lineages within the genus, and merits the status of a valid species.

As a rule for small didelphid marsupials, morphological variation in external and craniodental traits can be observed when large series are examined (Lemos & Cerqueira, 2002; Giarla, Voss & Jansa, 2010; Rossi *et al*., 2010b; Lóss *et al*., 2011; Pavan, Rossi & Schneider, 2012). Nevertheless, even when analysing a large series in the present study, the level of geographic variation found in several of the morphological traits did not obscure their diagnostic information. Indeed, the congruence between molecular, morphological, and morphometric data strongly supports the revalidation of *G. peruanus*.

In terms of the external and craniodental morphology, the most similar species with *G. peruanus* is *G. agilis*, which was, until now, considered its senior synonym. As previously observed, *G. agilis* exhibits notable dorsal pelage colour variation, ranging from dusky grey to dull reddish brown, according to Creighton

Table 11. Variation of craniodental morphology[a] among species of *Gracilinanus* examined in this study

	C1 accessory cusps		Posterolateral palatal foramen in relation to the palatine fenestra			Morphology of the anteromedial process of the alisphenoid tympanic process		
Species	Absent	Present	Smaller	Similar	Larger	Narrow	Median	Wide
Gracilinanus aceramarcae	1 (100%)	_	_	_	1 (100%)	_	_	1 (100%)
Gracilinanus agilis	65 (95%)[b]	3 (5%)[b]	11 (21%)	11 (21%)	29 (58%)	57 (91%)	5 (9%)	0 (0%)
Gracilinanus dryas	1 (25%)[c]	3 (75%)[c,e]	4 (100%)	–	–	–		4 (100%)
Gracilinanus emiliae	_	2 (100%)	2 (100%)	_	_	_	_	2 (100%)
Gracilinanus marica	1 (16,5%)[d]	5 (83,5%)[d,e]	–	1 (16,5%)	5 (83,5%)	–	–	6 (100%)
Gracilinanus microtarsus	7 (87,5%)	1 (12,5%)	6 (75%)	2 (25%)	_	5 (62,5%)	3 (37,5%)	_
Gracilinanus peruanus	31 (46%)[f]	34 (54%)[g]	37 (62%)	19 (31%)	4 (7%)	12 (18%)	30 (47%)	23 (35%)

[a]See text for trait definitions.

[b]Voss *et al*. (2009) treated as usually absent. Voss *et al*. (2005) examined 30 specimens from San Joaquin, Beni, Bolivia, and found no evidence of this trait in this series [Hershkovitz (1992) reported variation on this character for the same sample, but Voss *et al*. (2005) showed that the specimens cited by Hershkovitz that lack this trait are now referable to *Cryptonanus unduaviensis*].

[c]Voss *et al*. (2005: table 3) scored the craniodental trait frequencies for seven specimens of *Gracilinanus dryas* [BMNH 98.5.15.2 (holotype); USNM 372924–372926, 385017, 385018, 418517], five of which did not exhibit accessory cusps in C1. Similarly, Voss *et al*. (2009: table 1) mentioned the absence of accessory cusps in C1 for *Gracilinanus dryas*; however, we have examined four specimens of *G. dryas*, including the holotype, and three of them showed accessory cusps in C1 (BMNH 98.5.15.2, 98.7.1.26, 98. 7.1.27).

[d]Voss *et al*. (2005) examined 12 specimens of *Gracilinanus marica* [AMNH 21319, 21324, 21329, 21331, 21332, 24321, 24325, 24326, 206763; BMHN 98.5.15.1 (holotype); USNM 280881 (holotype of *Gracilinanus perijae*), 280884] and none of them showed accessory cusps in C1. By contrast, we examined six specimens, five of which exhibited accessory cusps in C1.

[e]The accessory cusps in C1 found in *Gracilinanus dryas* and *Gracilinanus marica* are smaller and smoother when compared with the accessory cusps in C1 found in *Gracilinanus emiliae* and *Gracilinanus peruanus*. These may account for the dissimilarities found between the analysis in this work and that of Voss *et al*. (2005, 2009) for this trait.

[f]Mature adult specimens with worn upper canines.

[g]Usually young adult specimens with unworn upper canines.

& Gardner (2008); however, we observed that this pelage variation is taxonomically informative, as side-by-side comparisons revealed that specimens with reddish brown dorsal fur refer to *G. peruanus*, whereas those with brownish/greyish tones refer to *G. agilis*. Furthermore, we found that adult specimens of both species can be consistently distinguished by the relative position of the anterior margin of the maxillary fenestrae, and to a lesser extent by the presence/absence of accessory cusps in the upper canine and by the morphology of the alisphenoid tympanic process.

Most of the craniodental dimensions overlapped between these species, so they cannot be used as reliable diagnostic traits; however, in most craniodental dimensions, *G. agilis* is significantly larger than *G. peruanus*, as shown by Student's *t*-tests (Table 5). These tests also demonstrated sexual dimorphism in several craniodental dimensions for both species, with males averaging larger than females, as previously reported for *G. agilis* and *G. microtarsus* (Costa *et al*., 2003; Fernandes *et al*., 2010), and other Neotropical didelphid marsupials (Mustrangi & Patton, 1997; Lew, Perez-Hernandez & Ventura, 2006; Astúa, 2010; Rossi *et al*., 2010b; Pavan *et al*., 2012).

The collecting localities of *G. peruanus* comprise central Peru, central Bolivia, and western Brazil in the states of Rondônia and north-western Mato Grosso, and encompass several ecoregions; *G. peruanus* inhabits both dry and moist forested areas, and is able to use gallery forests to enter savanna-like formations in the Brazilian Cerrado. Similar distributional patterns have also been reported for other didelphid marsupials, such as *Caluromys lanatus* (Olfers, 1818), *Didelphis marsupialis* Linnaeus, 1758, *Marmosops bishopi* (Pine, 1981), *Marmosops noctivagus* (Tschudi, 1845), and *Philander opossum canus* (Osgood, 1913)

Figure 11. Gallery forest where *Gracilinanus peruanus* and *Gracilinanus agilis* were found in sympatry (locality 3 in Fig. 1). Note the black arrow showing the deforested area near the trapping site. Photo courtesy of Vitor Azarias.

Table 12. Morphological variation of the circumocular mask in *Gracilinanus agilis* and *Gracilinanus peruanus*

	Circumocular mask	
Species	Poorly developed	Developed
Gracilinanus agilis	67 (92%)	6* (8%)
Gracilinanus peruanus	32 (94%)	2† (6%)

*Specimens from eastern Mato Grosso state, Brazil.
†The holotype (BMNH 27.11.1. 268) and topotype (BMNH 27.11.1.269) of *Marmosa agilis peruana*.

(Patton & Costa, 2003; Gardner & Creighton, 2008). The species in the genus *Gracilinanus* that is more associated with open formations is *G. agilis*, with the other species of the genus (including *G. peruanus*) being more associated with forested formations (Voss *et al*., 2009; Carmignotto, Vivo & Langguth, 2012). The presence of *G. agilis* in Peru, as previously reported by Creighton & Gardner (2008) and Huamaní, Cadenillas & Pacheco (2009), still needs to be confirmed by future analyses of the vouchers reported by authors. These analyses are also necessary to fill the distributional gaps and to provide important information on the natural history and habitat requirements of the poorly studied species of *Gracilinanus*.

The contiguous area formed by eastern Bolivia and central–western Brazil merits the attention of taxonomists, phylogeographers, and conservationists, as it harbours a high diversity of small mammals and is subject to an accelerated deforestation process for agriculture and cattle ranching developments (Yoshikawa & Sanga-Ngoie, 2011). Among the species recently described or recorded for the area mentioned, several are associated with the Chiquitano dry forest such as *Marmosops ocellatus* (Semedo, Rossi & Santos Júnior, 2013), whereas others are less restricted in terms of ecoregions, such as *Hylaeamys acritus* (Emmons & Patton, 2005) and *Oecomys sydandersoni* Carleton, Emmons & Musser, 2009. This area also harbours species mainly associated with the Amazon forests, such as *Glironia venusta* Thomas, 1912 (Rossi *et al*., 2010a).

Finally, it is important to note that the geographic ranges of *G. agilis* and *G. peruanus* partially overlap, as shown by the records of the former species in localities 33 and 45, and the records of sympatry in localities 3 and 15 (Fig. 1). As a result, ecological studies are necessary to assess whether these species are sharing the same ecological niches in these localities or whether there is a degree of interbreeding present.

The diversity within the genus *Gracilinanus* is still underestimated, and because of its geographically widespread distribution in South America, this genus is certainly an interesting group for biogeographic and

evolutionary studies. Additional inventory, morphological, and molecular studies are needed to assess the geographic distributional limits of the species within the genus, to uncover its hidden diversity (possibly cryptic species), and to understand the factors involved in the evolution of this poorly studied genus.

ACKNOWLEDGEMENTS

We are grateful to the following curators and collection managers for permitting access to specimens under their care: Robert Voss (AMNH), Roberto Portela (BMNH), Tereza Cristina (CM), João Alves (MN), Norka Rocha (MNK), Suely Marques-Aguiar (MPEG), Mario de Vivo and Juliana Gualda (MZUSP), and Pedro Cordeiro (UFPB). We also thank T. Hrbek for designing the primers used in this study; G. Libardi for helping with the morphometric analyses; and C.L. Miranda for analysing specimens in the MPEG. This study was supported by the Fundação de Amparo à Pesquisa do Estado de Mato Grosso (FAPEMAT, #567000/2008 and #477017/2011 to R.V.R.); Conselho Nacional de Desenvolvimento Científico e Tecnológico (CNPq, #552032/2010-7 to R.V.R., coordinated by C.Y. Nagamachi; Rede BioPHAM/CNPq 554057/2006-9 to I.P.F.); Fundação de Amparo à Pesquisa do Estado do Pará (FAPESPA, ICAAF 007/2011 to R.V.R., coordinated by C.Y. Nagamachi); Fundação do Estado do Amazonas (FAPEAM to I.P.F.); and Fundação de Amparo à Pesquisa do Estado de São Paulo (FAPESP, #2010/03969-4 to M.V.B and #2011/20022-3 to A.P.C). T.B.F.S., R.V.R., and I.P.F. were supported by a fellowship from CNPq, Brazil. Finally, we thank Robert S. Voss and one anonymous referee for helpful suggestions for the article.

REFERENCES

Anderson S. 1993. Los mamíferos bolivianos: notas de distribuición y claves de identificación. *Publ. Espec. Inst. Ecol.* (Colecc. Boliviano de Fauna), 159 pp.

Astúa D. 2010. Cranial sexual dimorphism in New World marsupials and a test of Rensch's rule in Didelphidae. *Journal of Mammalogy* **91:** 1011–1024.

Brown SDJ, Collins RA, Boyer S, Lefort M-C, Malumbres-Olarte J, Vink CJ, Cruickshank RH. 2012. Spider: an R package for the analysis of species identity and evolution, with particular reference to DNA barcodinG. *Molecular Ecology Resources* **12:** 562–565. doi: 10.1111/j.1755-0998.2011.03108.x.

Burmeister H. 1854. *Systematische uebersicht der thiere Brasiliens, welche während einer reise durch die Provinzen von Rio de Janeiro and Minas Geraes gesammelt oder beobrachetet wunden*. Erster theil, Säugethiere. Berlin, *G. Reimer*. 342 pp.

Cabrera A. 1958 ('1957'). Catálogo de los mamíferos de América del Sur [part 1]. *Revista del Museo Argentino de Ciencias Naturales 'Bernardino Rivadavia' e Instituto Nacional de Investigación de las Ciencias Naturales Zoologia* **4:** 1–307.

Carleton MD, Emmons LH, Musser GG. 2009. A new species of the rodent genus *Oecomys* (Cricetidae: Sigmodontinae: Oryzomyini) from eastern Bolivia, with emended definitions of *O. concolor* (Wagner) and *O. mamorae* (Thomas). *American Museum Novitates* **3661:** 1–32.

Carmignotto AP, Vivo M, Langguth A. 2012. Mammals of the Cerrado and Caatinga. Distribution patterns of the tropical open biomes of central South America. In: Patterson BD, Costa LP, eds. *Bones, Clones, and Biomes. The history and geography of Recent Neotropical mammals*. Chicago, IL: Chicago University Press, 307–350.

Costa LP, Leite YLR, Patton JL. 2003. Phylogeography and systematic notes on two species of gracile mouse opossums, genus *Gracilinanus* (Marsupialia: Didelphidae) from Brazil. *Proceedings of the Biological Society of Washington* **116:** 275–292.

Creighton GK, Gardner AL. 2008 ('2007'). Genus *Gracilinanus* Gardner and Creighton, 1989. In: Gardner AL, ed. *Mammals of South America, vol.* 1. Chicago, IL: University of Chicago, 43–50.

D'Elía G, Martínez JA. 2006. Registros uruguayanos de *Gracilinanus* Gardner y Creighton, 1989 y *Cryptonanus* Voss, Lunde y Jansa, 2005 (Didelphimorphia, Didelphidae). *Mastozoologia Neotropical* **3:** 245–249.

Diaz MM, Flores DA, Barquez RM. 2002. A new species of Gracile mouse opossum, genus *Gracilinanus*, from Argentina. *Journal of Mammalogy* **83:** 824–833.

Emmons LH, Patton JL. 2005. A new species of *Oryzomys* (Rodentia: Muridae) from eastern Bolivia. *American Museum Novitates* **3478:** 1–26.

Faria MB, Nascimento FF, Oliveira JA, Bonvicino CR. 2013. Biogeographic Determinants of Genetic Diversification in the Mouse Opossum *Gracilinanus agilis* (Didelphimorphia: Didelphidae). *Journal of Heredity* **104:** 613–626.

Fernandes FR, Cruz LD, Martins EG, dos Reis SF. 2010. Growth and home range size of the gracile mouse opossum *Gracilinanus microtarsus* (Marsupialia: Didelphidae) in Brazilian cerrado. *Journal of Tropical Ecology* **26:** 185–192.

Gardner AL. 1993. Order Didelphimorphia. In: Wilson DE, Reeder DM, eds. *Mammal species of the world a taxonomic and geographic reference*. Washington, DC: Smithsonian Institute Press, 15–23.

Gardner AL, Creighton GK. 1989. A new generic name for Tate's (1933) *microtarsus* group of South-American mouse opossums (Marsupialia, Didelphidae). *Proceedings of the Biological Society of Washington* **102:** 3–7.

Gardner AL, Creighton GK. 2008 ('2007'). Genus *Marmosops* Matschie, 1916. In: Gardner AL, ed. *Mammals of South America, Volume I. marsupials, xenarthrans, shrews, and bats*. Chicago, IL and London: University of Chicago Press, 61–74.

Giarla TC, Voss RS, Jansa SA. 2010. Species limits and phylogenetic relationships in the didelphid marsupial genus *Thylamys* based on mitochondrial DNA sequences and morphology. *Bulletin of the American Museum of Natural History* **346:** 1–67.

Gutiérrez EE, Jansa SA, Voss RS. 2010. Molecular systematics of mouse opossums (Didelphidae: *Marmosa*): assessing species limits using mitochondrial DNA sequences, with comments on phylogenetic relationships and biogeography. *American Museum Novitates* **3692:** 1–22.

Hall TA. 1999. BioEdit: a user-friendly biological sequence alignment editor and analysis program for Windows 95/98/NT. *Nucleic Acids Symposium Series* **41:** 95–98.

Hershkovitz P. 1992. The South American gracile mouse opossum, genus *Gracilinanus* Gardner and Creighton, 1989 (Marmosidae, Marsupialia): a taxonomic review with notes on general morphology and relationships. *Fieldiana Zoology* **70:** 1–55.

Huamaní L, Cadenillas R, Pacheco V. 2009. First record of *Gracilinanus agilis* (Burmeister, 1854) (Mammalia: Didelphidae) for Loreto, Peru. *Revista Peruana de Biologia.* **16:** 219–220.

ICZN. 1999. *International code of zoological nomenclature*, *4th edn*. Adopted by the International Union of Biological Sciences. London: The International Trust for Zoological Nomenclature, xxix. + 306 pp.

Jobb G, von Haeseler A, Strimmer K. 2004. TREEFINDER: a powerful graphical analysis environment for molecular phylogenetics. *BMC Evolutionary Biology* **4:** 18.

Kimura MA. 1980. Simple method for estimating evolutionary rates of base substitutions through comparative studies of nucleotide-sequences. *Journal of Molecular Evolution* **16:** 111–120.

Langguth A, Limeira VLAG, Franco S. 1997. Nuevo catálogo do material tipo da coleção de mamíferos do Museu Nacional. *Publicações Avulsas do Museo Nacional, Rio de Janeiro* **70:** 1–29.

Lemos B, Cerqueira R. 2002. Morphological differentiation in the white-eared opossum group (Didelphidae: *Didelphis*). *Journal of Mammalogy* **83:** 354–369.

Lew D, Perez-Hernandez R, Ventura J. 2006. Two new species of *Philander* (Didelphimorphia, Didelphidae) from northern South America. *Journal of Mammalogy* **87:** 224–237.

Lóss S, Costa LP, Leite YLR. 2011. Geographic variation, phylogeny and systematic status of *Gracilinanus microtarsus* (Mammalia: Didelphimorphia: Didelphidae). *Zootaxa* **2761:** 1–33.

Miranda-Ribeiro A. 1936. Didelphia ou Mammalia-Ovovivipara. *Revista Museu Paulista, São Paulo* **20:** 246–427.

Miranda-Ribeiro P. 1955. Tipos das espécies e subespécies do Prof. Alípio de Miranda-Ribeiro depositados no Museu Nacional. *Arquivos Museu Nacional, Rio de Janeiro* **42:** 389–417.

Mustrangi MA, Patton JL. 1997. Phylogeography and systematics of the slender opossum *Marmosops* (Marsupialia, Didelphidae). *University of California Publications in Zoology* **130:** 1–86.

Olson DM, Dinerstein E, Wikramanayake ED, Burgess ND, Powell GVN, Underwood EC, D'Amico JA, Itoua I, Strand HE, Morrinson JC, Loucks CJ, Allnutt TF, Ricketts TH, Jura Y, Lamoreux JF, Wettengel WW, Hedao P, Kassem KR. 2001. Terrestrial ecoregions of the world: a new map of life on Earth. *BioScience* **51:** 933–938.

Patton JL, Costa L. 2003. Molecular phylogeography and species limits in rainforest didelphid marsupials of South America. In: Jones ME, Dickman CR, Archer M, eds. *Predators with pouches: the biology of carnivorous marsupials*. Melbourne: CSIRO Press, 63–81.

Pavan SE, Rossi RV, Schneider H. 2012. Species diversity in the *Monodelphis brevicaudata* complex (Didelphimorphia: Didelphidae) inferred from molecular and morphological data, with the description of a new species. *Zoological Journal of the Linnean Society* **165:** 190–223.

Paynter JR, Traylor JRMA. 1991. *Ornithological gazetteer of Brazil*. Cambridge, MA: Museum of Comparative Zoology.

Posada D. 2006. ModelTest Server: a web-based tool for the statistical selection of models of nucleotide substitution online. *Nucleic Acids Research* **34:** W700–W703.

Posada D. 2009. Selection of models of DNA evolution with jModelTest. In: Posada D, ed. *Bioinformatics for DNA sequence analysis*. Methods in Molecular Biology Series. New York: Humana Press, 93–112.

Ronquist F, Teslenko M, van der Mark P, Ayres DL, Darling A, Höhna S, Huelsenbeck JP. 2012. MrBayes 3.2: efficient Bayesian phylogenetic inference and model choice across a large model space. *Systematic Biology* **61:** 539–542. doi:10.1093/sysbio/sys029.

Rossi RV, Miranda CL, Santos TS, Semedo TBF. 2010a. New records and geographic distribution of the rare *Glironia venusta* (Didelphimorphia, Didelphidae). *Mammalia* **74:** 445–447.

Rossi RV, Voss RS, Lunde DPA. 2010b. Revision of the didelphid marsupial genus *Marmosa*. Part 1. The species in Tate's 'Mexicana' and 'Mitis' sections and other closely related forms. *Bulletin of the American Museum of Natural History* **334:** 1–83.

Sambrook JF, Ritsch EF, Aniatis MT. 1989. *Molecular cloning: a laboratory manual*, *2nd edn*. Cold Spring Harbor, NY: Cold Spring Harbor Laboratory Press.

Semedo TBF, Rossi RV, Santos Júnior TS. 2013. New records of the Spectacled Slender Opossum *Marmosops ocellatus* (Didelphimorphia, Didelphidae) with comments on its geographic distribution limits. *Mammalia* **77:** 223–229.

Sokal RL, Rohlf FJ. 1981. *Biometry*, *2nd edn*. New York: W.H. Freemanand Company.

Swofford DL. 2002. *PAUP*: phylogenetic analysis using parsimony (*and other methods)*, *4th edn*. Sunderland, MA: Sinauer Associates.

Tamura K, Peterson D, Peterson N, Stecher G, Nei M, Kumar S. 2011. MEGA5: molecular evolutionary genetics analysis using maximum likelihood, evolutionary distance, and maximum parsimony methods. *Molecular Biology and Evolution* **28:** 2731–2739.

Tate GHH. 1931. Brief diagnoses of twenty-six apparently new forms of *Marmosa* (Marsupialia) from South America. *American Museum Novitates* **493:** 1–14.

Tate GHH. 1933. A systematic revision of the marsupial genus *Marmosa*. *Bulletin of the American Museum of Natural History* **66:** 1–250.

Teta P, Muschetto E, Maidana S, Bellomo C, Padula P. 2007. *Gracilinanus microtarsus* (Didelphimorphia, Didelphidae) en la Provincia de Misiones, Argentina. *Mastozoologia Neotropical* **14:** 113–115.

Thomas O. 1927. The Godman-Thomas Expedition to Peru. VI. On mammals from the Upper Huallaga and neighboring highlands. *Annals and Magazine of Natural History* Serie **20:** 594–608.

Vanzolini PE. 1992. A supplement to the Ornithological Gazetter of Brazil. São Paulo. *Museu de Zoologia da Universidade de São Paulo*, 252 pp.

Vieira COC. 1955. Lista remissiva dos mamíferos do Brasil. *Arquivos de Zoologia.* **8:** 341–474.

Voss RS, Fleck DWY, Jansa SA. 2009. On the diagnostic characters, ecogeographic distribution, and phylogenetic relationships of *Gracilinanus emiliae* (Didelphimorphia: Didelphidae: Thylamyini). *Mastozoología Neotropical* **16:** 433–443.

Voss RS, Jansa SA. 2003. Phylogenetic studies on didelphid marsupials II. Nonmolecular data and new IRBP sequences: separate and combined analyses of didelphine relationships with denser taxon samplinG. *Bulletin of the American Museum of Natural History* **276:** 1–82.

Voss RS, Jansa SA. 2009. Phylogenetic relationships and classification of didelphid marsupials, an extant radiation of New World metatherian mammals. *Bulletin of the American Museum of Natural History* **322:** 1–177.

Voss RS, Lunde DP, Jansa SA. 2005. On the contents of *Gracilinanus* Gardner and Creighton, 1989, with the description of a previously unrecognized clade of small didelphid marsupials. *American Museum Novitates* **3482:** 1–34.

Voss RS, Lunde DP, Simmons NB. 2001. The mammals of Paracou, French Guiana: a Neotropical lowland rainforest fauna. Part 2, nonvolant species. *Bulletin of the American Museum of Natural History* **263:** 1–236.

Voss RS, Tarifa T, Yensen E. 2004. An introduction to *Marmosops* (Marsupialia: Didelphidae) with the description of a new species from Bolivia and notes on the taxonomy and distribution of other Bolivian forms. *American Museum Novitates* **3466:** 1–40.

Yoshikawa AS, Sanga-Ngoie K. 2011. Deforestation dynamics in Mato Grosso in the southern Brazilian Amazon using GIS and NOAA/AVHRR data. *International Journal of Remote Sensing* **32:** 523–544.

APPENDIX

Gazetteer of examined and sequenced specimens

The localities of the examined and sequenced specimens of *Gracilinanus* included in this study are listed below. Numbers correspond to specimen records plotted on the map (Fig. 1). For each collecting locality (in bold), we provide the state or department, the corresponding geographic coordinates, and the voucher examined. The geographic coordinates were transcribed from voucher tags or obtained from the literature (Paynter & Traylor, 1991; Hershkovitz, 1992; Vanzolini, 1992; Voss *et al*., 2009). Vouchers not examined in this study are cited with their reference. Underlined voucher numbers correspond to those with Cyt*b* sequences included in the molecular analysis.

Brazil

1. **Cachoeirão de Juruena**, Mato Grosso, 13°32′S, 58°48′W (UFMT 870, 872, 873, 876, 878: *Gracilinanus peruanus*).
2. **São João da Barra**, Mato Grosso, 10°19′S, 57°41′W (UFMT 1333: *G. peruanus*).
3. **Margem esquerda e direita do Rio Verde**, Mato Grosso, 12°48′S, 56°10′W (CM 592, 451, 455, 457, 459, 463, 464, 468, 469, 470, 489, 492: *G. peruanus*; CM 485, 486, 487: *G. agilis*). Locality of sympatry.
4. **Vila Bela de Santíssima Trindade**, Mato Grosso, 14°51′S, 59°57′W (MZUSP 35129: *G. peruanus*).
5. **Lambari d'Oeste**, Mato Grosso, 15°16′S, 57°46′W (MZUSP 35115: *G. peruanus*).
6. **Rio Sapezal**, Mato Grosso, 12°52′S, 58°41′W (MZUSP 35130: *G. peruanus*).
7. **Rio Juruena**, Mato Grosso, 13°12′S, 58°59′W (MZUSP 35123, 35124: *G. peruanus*).
8. **Rio Juruena**, Mato Grosso, 13°19′S, 59°02′W (MZUSP 35128: *G. peruanus*).
9. **Rio Juruena**, Mato Grosso, 13°04′S, 58°58′W (MZUSP 35128: *G. peruanus*).
10. **Rio Juruena**, Mato Grosso, 13°15′S, 59°02′W (MZUSP 35117: *G. peruanus*).
11. **Rio Juruena**, Mato Grosso, 12°59′S, 58°57′W (MZUSP 35111, 35112, 35113, 35125, 35126, 35127: *G. peruanus*).
12. **Vale de São Domingos**, Mato Grosso, 15°07' S, 58°57′W (MZUSP 35118–35122: *G. peruanus*).
13. **Rio Juruena**, Mato Grosso, 13°24′S, 59°00′W (MZUSP 35114: *G. peruanus*).
14. **Fazenda Quatro Meninas**, Mato Grosso, 15°20′S, 58°33′W (INPA 6741; MSF 921, 934, 953, 995, 975, 988, 998, 1012, 1038, 1054; *G. peruanus*).
15. **Fazenda Água Limpa**, Mato Grosso, 15°17′S, 58°37′W (INPA 6740, MSF 881, 906: *G. peruanus*; MSF 1154: *G. agilis*). Locality of sympatry.
16. **Fazenda Araputanga**, Mato Grosso, 15°21′S, 58°26′W (INPA 6738, 6739, MSF 228, 308, 344, 355, 356: *G. peruanus*).
17. **Fazenda Bandeirantes**, Mato Grosso, 15°22′S, 58°24′W (MSF 244, 251 257, 816: *G. peruanus*).
18. **Fazenda Alto Jauru**, Mato Grosso, 15°27′S, 58°26′W (INPA 6736, 6737, MSF 12, 15, 203, 207, 213, 216, 219: *G. peruanus*).
19. **Fazenda Canaã**, Mato Grosso, 15°27′S, 58°35′W (MSF 454, 816: *G. peruanus*).
20. **Fazenda Monte Fusco**, Mato Grosso, 15°32′S, 58°37′W (MSF 233, 261, 340, 341, 357, 358, 359, 360, 361: *G. peruanus*).

21. **Fazenda Pau D'Alho**, Mato Grosso, 15°22′S, 58°04′W (MSF 414: *G. peruanus*).
22. **Serra do Expedito**, Aripuanã, Mato Grosso 11°03′S, 59°30′W (UFMT 1379: *G. peruanus*).
23. **Chupinguaia**, Rondônia, 12°14′S, 60°44′W (UFMT 3816: *G. peruanus*).
24. **Município de Vilhena**, Rondônia, 12°43′S, 60°17′W (UFMT 1306: *G. peruanus*).
25. **APM Manso – Rio Casca**, Mato Grosso, 14°42′S, 56°16′ W (UFMT 461: *G. agilis*).
26. **Escola Evangélica Buriti**, Mato Grosso, 15°24′S, 54°48′W (UFMT 124: *G. agilis*).
27. **Fazenda Moreninha**, Mato Grosso, 15°20′S, 56°38′W (MSF 1056, 1067: *G. peruanus*).
28. **Fazenda Pouso Alegre**, Mato Grosso, 16°16′S, 56 38′W (UFMT 621: *G. agilis*).
29. **Fazenda Retiro Novo**, Mato Grosso, 16°22′S, 56°17′W (UFMT 683–693, 726, 729: *G. agilis*).
30. **RPPN Acurizal, Serra do Amolar**, Mato Grosso do Sul, 17°49′S, 57°33′W (MZUSP 35311, UFMT 1611, 1613: *G. agilis*).
31. **Base de Pesquisas do IBDF, Transpantaneira**, Mato Grosso, 17°07′S, 56°56′W (MZUSP 35309: *G. agilis*).
32. **PARNA Pantanal**, Mato Grosso, 17°51′S, 57°25′W (MZUSP 35185, 35186, 35187, 35188, 35189, 35190, 35191, 35192: *G. agilis*).
33. **Utiariti**, Rio Papagaio, Mato Grosso, 13°02′S, 58°17′W (MZUSP 12572: *G. agilis*).
34. **Fazenda Eldorado**, Barra do Graças, Mato Grosso, 15°35′S, 52°17′W (UFMT 2043, 2044: *G. agilis*).
35. **Mineração Caraíba**, Nova Xavantina, Mato Grosso, 14°38′S, 52°30′W (CM 382: *G. agilis*).
36. **Margem esquerda do Rio Cumbuco**, Primavera do leste, Mato Grosso, 15°13′S, 54°03′W (UFMT 1039: *G. agilis*).
37. **Jaciara/Jucimeira**, Mato Grosso, 16°07′S, 55°01′W (UFMT 3817, 3818: *G. agilis*).
38. **Rio Taquari**, Mato Grosso, 17°56′S, 53°23′W (MZUSP 35271–35274: *G. agilis*).
39. **Cocalinho**, Mato Grosso, 14°16′S, 50°59′W (MZUSP 35301–35306; *G. agilis*).
40. **Rio Garça**, Tesouro Mato Grosso, 16°01′S, 53°26′W (MZUSP 35275, 35276: *G. agilis*).
41. **Fazenda Espigão**, Itiquira, Mato Grosso, 15°20′S, 53°51′W (MZUSP 34697, 34706, 34707: *G. agilis*).
42. **Fazenda Araras**, Itiquira, Mato Grosso, 17°14′S, 53°41′W (MZUSP 34701, 34702, 34705: *G. agilis*).
43. **Toricoejo**, Rio das Mortes, Mato Grosso, 15°13′S, 53°10′W (MZUSP 35279–35297: *G. agilis*).
44. **Serra das Araras**, Mato Grosso, 15°39′S, 53°12′W (MZUSP 35307–35308: *G. agilis*).
45. **São José**, Mato Grosso, 13°27′S, 56°43′W (MZUSP 35300: *G. agilis*).
46. **Rio Garça**, Guiratinga, Mato Grosso, 15°37′S, 53°25′W (MZUSP 35277–35278: *G. agilis*).
47. **Rio Juruena**, Mato Grosso, 13°19′S, 59°2′W (MZUSP 35298, 35299: *G. agilis*).
48. **Alta Cachoeira**, Goiás, 18°43′S, 51°19′W (CM 598: *G. agilis*).
49. **Base de Pesquisas do Pantanal**, Mato Grosso, 17°07′S, 56°77′W, Costa *et al*. (2003), Lóss *et al*. (2011) (UFMG 2497: *G. agilis*).
50. **Chapada do Araripe**, Ceará, 07°17′S, 39°27′W, Costa *et al*. (2003), Lóss *et al*. (2011) (UFMG 2504; *G. agilis*).
51. **Floresta Nacional de Ipanema**, São Paulo, 23°26′S, 47°37′W, Lóss *et al*. (2011), type locality of *G. microtarsus* (UFMG 2537: *G. microtarsus*).
52. **Lagoa Santa**, Fazenda das Bicas, Minas Gerais, 19°38′S, 43°53′W, Lóss *et al*. (2011) (MN 31445: *G. microtarsus*).
53. **Lagoa Santa**, Sítio no Bairro Quebra, Minas Gerais, 19°38′S, 43°53′W (UFPB 2432: *G. microtarsus*).
54. **Riacho Grande**, São Bernardo do Campo, São Paulo, 23°42′S, 46°33′W (MZUSP 30641, 30745, 30752: *G. microtarsus*).
55. **Fazenda Intervales**, Capão Bonito, São Paulo, 24°20′S, 48°26′W (MZUSP 29159: *G. microtarsus*).
56. **Fragmento Zezinho**, Caucaia do Alto, São Paulo, 23°45′42″S 47°05′23″W (MZUSP 32659: *G. microtarsus*).
57. **Buri**, São Paulo, 23°48′S, 48°34′59″W (MZUSP 31009: *G. microtarsus*).
58. **Ilha dos Búzios**, São Paulo, 23°48′S, 45°08′W (MZUSP 12739: *G. microtarsus*).
59. **Ponte do Colatino**, Minas Gerais, 16°36′S, 42°12′W, Costa *et al*. (2003), Lóss *et al*. (2011) (UFMG 2495: *G. agilis*).
60. **Piraquara**, Paraná, 25°27′S, 49°04′W, Lóss *et al*. (2011) (MHNCI 2793: *G. microtarsus*).
61. **São João da Serra do Norte**, Rondônia, 12°44′S, 60°08′W, (MN 1276: *Thylamys rondoni*, paralectotype). The coordinates given by Hershkovitz (1992) are erroneous; we are using the coordinates provided by Vanzolini (1992).
62. **Fazenda Cachoeira**, Vilhena, Rondônia, 12°43′S, 60°17′W (MPEG 34925: *G. peruanus*).
63. **Ipuí**, Ceará, 04°20′S, 40°42′W (BMNH 11.4.23.24: *Marmosa agilis beatrix*, holotype).
64. **Near Belém**, Pará, 01°27′N, 48°29′W (BMNH 9.3.9.10: *G. emiliae*, holotype).
65. **São Bento**, Goiás, 18°27′S, 51°47′W (MN 1250: *Marmosa blaseri*, holotype).

BOLIVIA

66. **El Refugio**, Huanchaca, Santa Cruz, 14°46′S, 61°02′W (MNK 3744: *G. peruanus*).

67. **Buenavista**, Santa Cruz, 17°27′S, 63°21′W (BMNH 26.12.4.91: *Marmosa agilis buenavistae*, holotype).
68. **Rio Aceramarca**, La Paz, 16°18′S, 67°53′W (AMNH 72568: *Gracilinanus aceramarcae*, holotype).

PERU

69. **Nuevo San Juan**, Rio Galvez, Loreto, 05°15′S, 73°10′W, Voss *et al*. (2009), Giarla *et al*. (2010) (MUSM 15292: *G. emiliae*).
70. **La Convencion**, Cordillera de Vilcabamba, Junín, 11°40′S, 73°38′W, Costa *et al*. (2003), Lóss *et al*. (2011) (MUSM 13002: *G. aceramarcae*).
71. **Tingo Maria**, Huánuco, 09°08′S, 75°57′W (BMNH 27.11.1.268: *Marmosa agilis peruana*, holotype; BMNH 27.11.1.269: *M. a. peruana*, topotype).

VENEZUELA

72. **Rio Albarregas**, Mérida, 08°31′N, 71°09′W (BMNH 98.5.15.1: *G. marica*, holotype).
73. **Cafetales de Milla or Mérida**, Mérida, 08°36′N, 71°08′W (AMNH 21319, 21324, 21329, 21331: *G. marica*).
74. **Selva Culata**, Cordillera de Mérida, Mérida, 08°50′N, 71°00′W (BMNH 98.5.15.2: *G. dryas*, holotype).
75. **Uchisera**, Cordillera de Mérida, Mérida, 09°00′N, 71°00′W (BMNH 98.7.1.26, 98.7.1.27: *G. dryas*).
76. **Montes de la Serra**, Cordillera de Mérida, Mérida, 08°36′N, 41°08′W (BMNH 13.2.3.15: *G. dryas*).